UNIVERSITY OF
KWAZULU-NATAL

INYUVESI
YAKWAZULU-NATALI

The effect of patulin on adrenergic receptor signalling and DNA methylation in C57BL/6 mouse livers

By

Alisha Naidoo (220056048)

BSc. B. Med. Sc. (Hons) (UKZN)

Submitted in fulfillment of the requirements for the degree of

MASTER OF MEDICAL SCIENCE

In the Discipline of Medical Biochemistry
School of Laboratory Medicine and Medical Sciences,
College of Health Sciences
University of KwaZulu-Natal
Durban, South Africa

2024

Supervisors:

Professor Anil A. Chuturgoon & Dr Terisha Ghazi

Declaration

I, **Alisha Naidoo** declare that:

i. The research reported in this dissertation, except where otherwise indicated is my original work.

ii. This dissertation has not been submitted for any degree or examination at any other university.

iii. This dissertation does not contain other person's data, pictures, graphs, or other information unless specifically acknowledged as being sourced from other persons.

iv. This dissertation does not contain other persons writing unless specifically acknowledged as being sourced from other researchers. Where other sources have been quoted, then:

a. Their words have been rewritten but the general information attributed by them has been referenced.

b. Where their exact words have been used their writing has been placed inside quotation marks and referenced.

v. Where I have reproduced a publication of which I am the author, co-author, I have indicated in detail which part of the publication was written by myself alone and have fully referenced such publications.

vi. This dissertation does not contain text, graphics, or tables copied and pasted from the internet unless specifically acknowledged and the source is detailed in the dissertation and the reference sections.

Signed: [redacted] **Date:** 6/12/2024

Acknowledgements

I am eternally grateful to God for bestowing upon me the strength, courage and wisdom I need to achieve my goals. Thank you, God, for your guidance and blessings.

I thank my parents for your unwavering support and unconditional love which will always be my source of strength. Thank you for giving me everything that I could ever need and making everything a possibility.

Thank you to my family for your support, understanding and for being constants.

To my supervisor, Dr Terisha Ghazi, thank you for always going the extra mile to assist me. You are an inspiration, and your teachings shall remain with me forever. It has been an honour to work under your supervision.

To my supervisor, Professor Anil. A. Chuturgoon, thank you for setting standards, inspiring us to attain more and propel the science field forward. I am grateful to have been supervised by you.

I thank you, my dear friends, for the laughs, support and help.

Thank you to the staff of the Biochemistry Department for all your help, motivation and pleasant conversations.

To the College of Health Sciences, a sincere thank you for funding this study.

Presentations

The effect of patulin on adrenergic receptor signalling and DNA methylation in C57BL/6 mouse livers.

1) School of Laboratory Medicine and Medical Sciences Proposal Defence Presentation, K-RITH, Medical School Campus, UKZN - 19th September 2024.

The effect of patulin on adrenergic receptor signalling and DNA methylation in C57BL/6 mouse livers.

2) School Laboratory Medicine and Medical Sciences Research Day, Senate Chambers, Westville Campus, UKZN - 27th September 2024.

Table of Contents

List of Figures

List of Tables

Abbreviations

5-caC	5-carboxylcytosine
5-fC	5-formylcytosine
5-HmC	5-hydroxymethylcytosine
5-mC	5-methylcytosine
α	Alpha
α-AR	Alpha-adrenergic receptor
α1A-AR	Alpha 1A-adrenergic receptor
α2A-AR	Alpha 2A-adrenergic receptor
α2B-AR	Alpha 2B-adrenergic receptor
γ	Gamma
AKT	Serine/threonine kinase/ protein kinase B
ALP	Alkaline phosphatase
ALT	Alanine aminotransferase
Ahcy	Adenosylhomocysteinase hydrolase
ARRIVE	Animal research: reporting of *in vivo* experiments
AR	Adrenergic receptor
APS	Ammonium persulfate
AST	Aspartate aminotransferase
BAD	B-cell lymphoma 2 associated agonist of cell death
BCL 2	B-cell lymphoma 2

BCA	Bicinchoninic acid
β	Beta
β-AR	Beta-adrenergic receptor
β1-AR	Beta 1-adrenergic receptor
β2-AR	Beta 2-adrenergic receptor
β3-AR	Beta 3-adrenergic receptor
BW	Body weight
BSA	Bovine serum albumin
CA	California
CAT	Catalase
CH_3	Methyl group
Ct	Comparative threshold
Cys	Cysteine
cDNA	Complementary DNA
CpG	Cytosine-phosphate-guanine
dH_2O	Distilled water
dNTPs	Deoxynucleotide triphosphates
DNA	Deoxyribonucleic acid
DNMT	DNA methyl transferase
DNMT 1	DNA methyl transferase 1
DNMT 3A	DNA methyl transferase 3A

DNMT 3B	DNA methyl transferase 3B
dT	Deoxythymidine
ELISA	Enzyme-linked immunosorbent assay
ERK	Extracellular signal-regulated kinase
EU	European Union
GAPDH	Glyceraldehyde-3-phosphate dehydrogenase
GPCRs	G protein-coupled receptors
Glu	Glutamic acid
GR	Glutathione reductase
GRB-2	Growth factor receptor-bound protein 2
GSH	Glutathione
GPx	Glutathione peroxidase
GSK3β	Glycogen synthase kinase-3 beta
HEK293	Human embryonic kidney
Hr	Hour
H_2O_2	Hydrogen peroxide
IARC	International Agency for Research on Cancer
IP3	Inositol triphosphate
JNK	Jun N-terminal kinase
Lys	Lysine
MA	Massachusetts

MAPK	Mitogen-activated protein kinases
MBD	Methyl-CpG-binding domain
MBD-2	Methyl-CpG-binding domain protein 2
MDA	Malondialdehyde
miR	MicroRNA
mRNA	Messenger RNA
mTOR	Mammalian target of rapamycin
mTORC2	Mammalian target of rapamycin complex 2
MDM2	Mouse double minute 2 homolog
Na^+	Sodium
NaOH	Sodium hydroxide
NAFLD	Non-alcoholic fatty liver disease
PAT	Patulin
PBS	Phosphate-buffered saline
PCR	Polymerase chain reaction
PDK	Phosphoinositol-dependent kinase
Phe	Phenylalanine
PH	Pleckstrin homology
PIP_2	Phosphatidylinositol 1, 2-biphosphate
PIP_3	Phosphatidylinositol (3, 4, 5)-phosphate
PI3K	Phosphatidylinositol-3-kinase

PKB	Protein kinase B
PKC	Protein kinase C
PLC	Phospholipase C
PTEN	Phosphatase and tensin homolog
qPCR	Quantitative polymerase chain reaction
Raf-1	Rapidly accelerated fibrosarcoma-1
RAS	Rat sarcoma
RBD	Relative band density
Rpn4	Regulatory particle non-ATPase 4
ROS	Reactive oxygen species
RT	Room temperature
RTKs	Receptor tyrosine kinases
SOD	Superoxide dismutase
SAH	S-adenosylhomocysteine
SAM	S-adenosylmethionine
Ser	Serine
Shc	Src homology and collagen
SDS	Sodium dodecyl sulphate
SDS-PAGE	Sodium dodecyl sulfate-polyacrylamide gel electrophoresis
SNS	Sympathetic nervous system
SOS	Son of sevenless proteins

Taq	Thermus aquaticus
TET	Ten-eleven translocation
TET 1	Ten-eleven translocation 1
TET 2	Ten-eleven translocation 2
TET 3	Ten-eleven translocation 3
TE	Tris-EDTA
TEMED	Tetramethylethylenediamine
Thr	Threonine
TM	Transmembrane
TTBS	Tris buffer saline with Tween 20
Tyr	Tyrosine
UK	United Kingdom
USA	United States of America
UTR	Untranslated region

Abstract

Background: Secondary metabolic products of fungi and mould are called mycotoxins, and they are usually hazardous to organisms. Patulin (PAT) is a mycotoxin most prevalent in apples and their products, such as juice and cider. PAT may threaten animal and human health by causing chronic effects including immunotoxicity, genotoxicity, teratogenicity, and carcinogenicity. Research demonstrates that PAT is hepatotoxic; however, its mechanism of action is unclear. The adrenergic receptors are altered during liver injury. The adrenergic receptors utilise the mitogen- activated protein kinases/extracellular signal-regulated kinase (MAPK/ERK) and phosphatidylinositol-3-kinase/protein kinase B (PI3K/AKT) pathways. It is unclear if ARs are modulated by DNA methylation. DNA methylation is crucial for cell differentiation. Hence its dysregulation can lead to diseases such as cancer.

Aim: To determine the effect of PAT on global DNA methylation and adrenergic receptor signalling in C57BL/6 mouse livers.

Methods: In the livers of four C57BL/6 mice fed PAT (2.5 mg/kg BW) for 10 days: qPCR determined the mRNA expression of *alpha* and *beta-adrenergic receptors*, as well as *MAPK, MAPK14, ERK1/2, PI3K and AKT, DNMT1, DNMT3A, DNMT3B and MBD2*. Western blot determined the protein expression of P38, ERK1/2, PI3K, DNMT1, DNMT3A, and MBD2. The ELISA assay was used to determine global DNA methylation levels.

Results: PAT significantly increased *alpha-1A adrenergic receptor* mRNA levels whilst decreasing *alpha-2A, 2B,* and all *beta-adrenergic receptor* expression, with *beta-2* reduced significantly. *PI3K's* decline was PAT-induced. PAT significantly increased *AKT, MAPK, MAPK14,* and *ERK1* expression but significantly reduced *ERK2* levels. PAT increased *MBD2* and *DNMT1* expression while significantly decreasing *DNMT3A* and *3B* levels. PAT significantly increased and decreased the protein levels of P38 and ERK1/2 respectively. Additionally, a PAT- mediated increase in PI3K protein levels was observed. PAT significantly increased DNMT1 and increased DNMT3A and MBD2 expression. Significant global hypermethylation was PAT- induced.

Discussion/Conclusion: PAT significantly impacted alpha-1A and beta-2 adrenergic receptors which also utilise the MAPK/ERK/PI3K/AKT pathway. The dysregulation of these signalling cascades has been associated with altered expression of the adrenergic receptors. PAT-induced global hypermethylation. PAT disrupts adrenergic receptor signalling and modifies global DNA methylation, thus resulting in liver injury.

Keywords: patulin, adrenergic receptors, MAPK/ERK/PI3K/AKT, global DNA methylation, hepatotoxicity.

Chapter 1: Introduction

Fungal secondary metabolic products known as mycotoxins are toxic to organisms (Awuchi et al., 2022a). Climate conditions, pest infestation, and improper harvesting and storage procedures are conducive to fungal contamination and mycotoxin production in food. The Food and Agriculture Organisation (FAO) reports that mycotoxin contamination affects almost 25% of agricultural products globally (World Health, 2011). When consumed at excessive doses, mycotoxins can lead to acute poisoning and even death (World Health, 2023). Due to their severe toxicity, mycotoxins have gained attention in the past decade (World Health, 2023). Mycotoxins of agricultural importance include fumonisins, aflatoxins, ochratoxins, and patulin (PAT) (Saleh and Goktepe, 2019).

Aspergillus, Byssochlamys and Penicillium fungal species predominantly generate PAT (Torović et al., 2017). PAT ($C_7H_6O_4$; 154.12 g/mol) is a water-soluble white powder that contains a polyketide lactone structure (Iqbal et al., 2018, Saleh and Goktepe, 2019). PAT has been detected across the globe (Saleh and Goktepe, 2019). The primary route of exposure to PAT is through ingestion of contaminated foods (Duncan et al., 2021). While PAT is found in fruits and vegetables, it is predominantly present in apples (Zhong et al., 2018). *Penicillium expansum* produces the hazardous mycotoxin PAT, which causes “blue mould” in damaged apples (Hammami et al., 2017). According to a study by Bissessur et al. PAT's electrophilic properties may allow it to attach to the solid part of apples (Bissessur et al., 2001). The chemical purification process cannot detect PAT once it’s bound (Saleh and Goktepe, 2019). PAT poses significant health concerns for humans and animals (Chu et al., 2021). PAT induces acute, and chronic toxicity (Torović et al., 2017). Acute symptoms encompass a range of conditions such as vomiting, ulcers, agitation, inflammation of the intestines, and convulsions (Iqbal et al., 2018). In rat models, subacute toxicity was characterised by weight loss, impaired kidney function, hindering numerous enzymes, and gastrointestinal disturbances defined by distension and bleeding. Chronic symptoms comprise genotoxic, carcinogenic, developmental, and organ-specific, toxic effects (Qiu et al., 2022).

Adrenergic receptors (AR) are class A G protein-coupled receptors classified under the rhodopsin family, which regulate epinephrine and norepinephrine activity (Wu et al., 2021). The two types

of adrenoreceptors: alpha and beta are further classified into subtypes such as α1A- AR, α1B-AR, α1D-AR, α2A-AR, α2B-AR, α2C-AR, β1-AR, β2-AR, and β3-AR (Chen et al., 2020). The α-AR and β-AR serve crucial roles in the liver. The α1A and α2A-AR regulate inflammation in the Kupffer cells whilst α2B-AR regulates liver fibrosis (Huan et al., 2017, Schwinghammer et al., 2020). The β1 governs hepatic norepinephrine-mediated pro-inflammatory response (Zapater et al., 2012). The β2-AR promotes liver regeneration (Tao et al., 2022). The β3-AR expression increases significantly in human and rat cirrhosis liver (Trebicka et al., 2009).

Upon its conformational activation, α1-AR engages with Gq/proteins and activates phospholipase C (PLC). PLC converts phosphatidylinositol 1, 2-biphosphate (PIP_2) to inositol triphosphate (IP3) and diacylglycerol (DAG), which releases intracellular calcium (Ca^{2+}). Smooth muscle contractions and protein kinase C (PKC) stimulated by DAG and Ca^{2+}. PKC ensures proteins are phosphorylated and mediate the proper response. This comprises mitogen-activated protein kinase (MAPK), and phosphatidylinositide-3-kinase (PI3K) (Pillay et al., 2020).

The α-ARs stimulate the MAPK/ERK and PI3K/AKT signalling cascades to trigger physiological effects (Mazibuko et al., 2024). Central to signalling networks, the MAPK/ERK cascade governs cell proliferation, development, and differentiation. Furthermore, this pathway modulates responses to stress (Guo et al., 2020). The PI3K/AKT signalling pathway influences cell growth, proliferation, metabolic processes and survival (Shamsan et al., 2024). This signalling cascade can reduce liver fibrosis (Shamsan et al., 2024).

Epigenetics is defined as inheritable gene alterations that do not alter DNA sequence and result in phenotypic modifications (Li et al., 2023). Epigenetics regulates cellular growth and differentiation. DNA methylation is a well-studied epigenetic mechanism that regulates genes. This reaction is catalysed by DNA methyltransferases (DNMTs) 1, 3A and 3B (Li et al., 2023). DNA demethylation levels are modulated by MBD2 (Kumar et al., 2018b). Research has demonstrated that mycotoxins alter DNA methylation patterns leading to harmful consequences (Li et al., 2023). The carcinogenicity of mycotoxins can be attributed to altered DNA methylation (Li et al., 2023).

1.1. Problem statement

Mycotoxin contamination is a worldwide concern that leads to various complications and unpleasant outcomes (Zheng et al., 2018). Moreover, mycotoxins have a significant economic impact on agriculture, resulting in annual financial losses worldwide (Pal et al., 2017). In Africa, food safety issues hinder food security, trading, and a healthy lifestyle. They contaminate food, feed and beverages. This affects the food chain and thus threatens human and animal health (Iqbal et al., 2024). Many disorders, particularly mycotoxicoses and mycoses, can result from mycotoxin ingestion, ultimately leading to mortality. PAT is prevalent globally (Saleh and Goktepe, 2019). The European Union (EU) set a maximum of 50 µg/kg of PAT in apple juice, 25 µg/kg in solid apple products, and 10 µg/kg in apple-based products for children and newborns (Iqbal et al., 2024). A South African study revealed that the mean concentration of PAT (210 µg/L) surpassed the established maximum threshold (Shephard et al., 2010). Particular age groups are more vulnerable to toxins. Pregnant women are at risk of toxin exposure, which can impact fetal development. Mothers on a plant-based diet with a higher daily fruit intake may be more susceptible to PAT exposure (Saleh and Goktepe, 2019). Nursing infants could be in danger if their mother is exposed to the maximum daily intake for adults or ingests a toxin that surpasses the safe limit for her age group (Saleh and Goktepe, 2019). PAT's prevalence in baby food, especially fruit juices, is a significant problem. Children are more susceptible than adults because they are exposed to higher levels of substances relative to their body weight and have distinct physiological traits (Saleh and Goktepe, 2019). Additionally, in mice, the offspring of PAT-exposed mothers were adversely affected, with mortality observed in males and females (Awuchi et al., 2022b). The primary route of mycotoxin exposure is through ingestion (Duncan et al., 2021). PAT toxicity primarily targets the liver (Chu et al., 2021). The liver is the first organ to receive PAT from the gut through enterohepatic circulation (Wei et al., 2020). It has demonstrated hepatotoxicity. However, the potential mechanisms are not entirely clear (Chu et al., 2021). Contrary to other mycotoxins, research on PAT is sparse and requires further exploration (Wei et al., 2020). Therefore, to fill this research gap, PAT's hepatotoxic mechanism utilising the adrenergic receptors, MAPK/ERK/PI3K/AKT pathways and global DNA methylation will be investigated.

1.2. Research questions

i. Does PAT affect alpha and beta-adrenergic receptor signalling in mouse livers?
ii. Does PAT alter alpha and beta-adrenergic receptors' mRNA and protein expression in mouse livers?
iii. Does PAT alter global DNA methylation levels in mouse livers?
iv. Does PAT alter the mRNA and protein expression of DNA methylation regulators including DNMT1, DNMT3A, DNMT3B and MBD2 mouse livers?

1.3. Aim

The study aims to determine the effect of PAT on adrenergic receptor signalling and global DNA methylation in C57BL/6 mouse livers.

1.4. Hypothesis

PAT alters adrenergic receptor signalling and global DNA methylation levels in mouse livers following prolonged exposure (10 days).

Confirmed hypothesis: The findings of the study proved the hypothesis to be true.

1.5. Objectives

- To determine global DNA methylation levels in the livers of C57BL/6 patulin fed mice using the enzyme-linked immunosorbent assay.
- To determine the mRNA expression of *alpha* and *beta-adrenergic receptors* as well as *MAPK, MAPK14, ERK1/2, PI3K* and *AKT, DNMT1, DNMT3A, DNMT3B* and *MBD2* in the livers of C57BL/6 patulin fed mice using the qPCR assay.
- To determine the protein expression of p38, ERK1/2, PI3K, DNMT1, DNMT3A and MBD2 in the livers of C57BL/6 patulin fed mice using the western blot assay.

Chapter 2: Literature review

2.1. Mycotoxins

Fungi produce secondary metabolites called mycotoxins (Chu et al., 2021). Fungi including *Aspergillus, Penicillium, Fusarium, and Rhizopus* produce mycotoxins (Nawaf, 2023). Mycotoxins have existed since the beginning of crop farming (Pal et al., 2017). Both internal and external environmental factors influence the production and release of mycotoxins. Some mycotoxins are produced primarily in the field, while others can develop both in the field and after harvesting (Awuchi et al., 2022b). They are commonly found in places with high temperatures and humidity, including tropical regions. Mycotoxins can be found in the spores or mycelium of fungi (Nawaf, 2023). Mycotoxins infiltrate the food chain when crops become infested with mould. They are chemically stable and can withstand the harsh conditions in the food supply chain (Awuchi et al., 2022b). Mycotoxin exposure can occur directly through the ingestion of infected feeds and foods, or indirectly when humans consume products from animals exposed to mycotoxin- contaminated feeds, such as milk, eggs and meat products. Aflatoxins, citrinin, ochratoxins, fumonisin, PAT, zearalenone, nivalenol, deoxynivalenol, and ergot alkaloids are among the most frequent mycotoxins affecting humans and livestock (Awuchi et al., 2022b). In humans and animals, mycotoxins are hepatotoxic, nephrotoxic, genotoxic, carcinogenic, neurotoxic and immune suppressors (Zheng et al., 2018, Duncan et al., 2021). The mycotoxin's toxic properties, amount, and duration of exposure determine the clinical manifestations. Mycotoxicoses refer to disorders produced by ingestion of mycotoxins (Nawaf, 2023). Through routes of exposure such as ingestion, inhalation, and skin contact, mycotoxicosis can induce acute and chronic effects in humans and livestock (Awuchi et al., 2022b). Studying mycotoxins' mechanism of action is vital as they weaken the host, thus allowing fungi to grow and inflict further damage (Awuchi et al., 2022b).

2.2. Patulin

2.2.1. History

PAT, a previously unknown metabolite of Penicillium patulum Bainier, was isolated and exhibited antibacterial characteristics. It was called anhydro-3-hydroxymethylene tetrahydro-y-pyrone-2-carboxylic acid (Raistrick, 1943). Chain et al. originally isolated PAT (4-hydroxy-4H-

furo[3,2-c] pyran-2(6H)-one) and named it claviformin as it was a *Penicillium claviforme* isolate (Chain et al., 1942). Claviformin was renamed as PAT after the PAT-producing mould, *Penicillium patulum* (which would later be called *P. urticae,* currently known as *P. griseofulvum*) that was extracted by Birkinshaw et al. (Birkinshaw et al., 1943). PAT had several names, including clavicin, clavitin, gigantic acid, expansin, leucopin, mycoin, penicidin, and tercinin. In the mid-1900s, PAT was recognised for its antibacterial and anticancer capabilities and as a medication to cure common colds from *Penicillium patulum* (Pal et al., 2017). As PAT suppresses gram-positive and gram-negative bacteria including Shigella species, E. coli and Salmonella typhi, earlier clinical research studied PAT's ability as an anti-bacterial agent (Wei et al., 2020). Between the years 1950 through 1960, PAT was re-identified as a mycotoxin although it has anti-bacterial, anti-viral, and anti-protozoal properties. In the 1960s, PAT was found to be highly toxic to bacteria and animals (Li et al., 2019).

2.2.2. Background

PAT is produced by fungi including *Aspergillus, Byssochlamys and Penicillium* (Chu et al., 2021). Various physiological variables, including temperature, moisture levels and storage conditions, influence PAT production. Additionally, acidic pH levels (3, 4 and 5) promote PAT production (Kumar et al., 2018a).

Humans are primarily exposed to PAT in apples and their products. Additionally, PAT can be found in decaying fruits including pears and strawberries as well as in various foods such as vegetables, cheese and cereals (Zheng et al., 2018) (Figure 2.1).

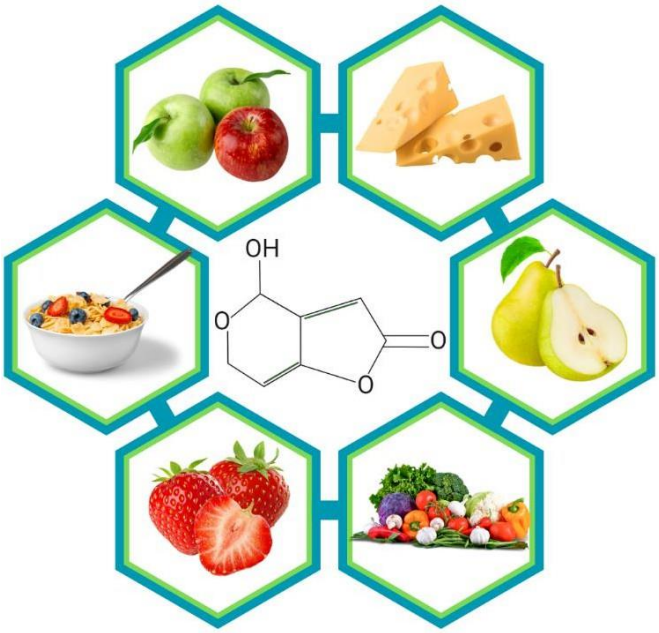

Figure 2.1: The various sources of PAT (prepared by author using canva.com).

Several studies conducted on apple juice reported the following concentrations of PAT. In a South African survey, the following PAT levels were found in apple juice: 5 out of 22 samples (23%) exhibited concentrations ranging from 10-45 ppb (Bissessur et al., 2001). Additionally, apple juice concentrates were obtained from three sources. All 215 samples contained concentrations of PAT between 7-375 ppb, and 43% of the samples surpassed the 50 ppb recommended threshold (Bissessur et al., 2001). In South Africa (Cape Town), 5 out of 8 samples of apple juice showed PAT levels exceeding 10 ng/ml, with one sample being substantially contaminated at 75 ng/ml (Katerere et al., 2007). In the United Kingdom, PAT was found in apple juice at 38 and 56 µg/kg (Leggott and Shephard, 2001).PAT tainted 23% of apple juice and cider samples where concentrations ranged from 8.8 to 2700.4 µg/L in Michigan, USA (Harris et al., 2009). The Czech Republic observed the presence of PAT in apples (415 µg/kg) (Vaclavikova et al., 2015). In Qatar (Doha), PAT contaminated all 20 samples of apple juice samples with concentrations ranging from 5.8-82.2 µg/kg (Hammami et al., 2017). In Beijing, 9 out of 23 apple juice samples were contaminated with PAT with levels ranging from 0.50-4.82 µg/L (Yang et al., 2017).

Out of 73 apple juice samples, 54 were affected by PAT in Serbia (Novi Sad) at levels < limit of quantification–65.4 (Torović et al., 2018). In Pakistan (Punjab), 15 out of 29 apple juice products displayed PAT contamination at < limit of quantification–120.5 µg/L (Iqbal et al., 2018). In Japan, apple juice products exhibited PAT contamination at a concentration of 464 µg/L (Li et al., 2019).

Other studies that tested infant products observed PAT contamination at the following levels. In SA, infant apple products displayed 29% contamination within 5-20 ppb (Bissessur et al., 2001). In Qatar (Doha), all 6 infant apple juice samples tested positive for PAT with concentrations ranging from 7.7-61.3 µg/kg (Hammami et al., 2017). Interestingly, studies conducted on other fruits found PAT contamination at the following levels. The Czech Republic observed the presence of PAT in various products, pears (41.6 µg/kg) and a fruit salad mix (14 µg/kg) (Vaclavikova et al., 2015). In Pakistan (Punjab), grapes contained PAT at levels ranging from 410-1100 µg/kg (Iqbal et al., 2018). Furthermore, in Cameroon, the level of PAT-contaminated maize-*fufu* samples ranged from 12-890 µg/kg with a mean of 105 µg/kg (Abia et al., 2017). Based on these statistics, it is evident that PAT is a global concern.

2.2.3. Patulin's structure

PAT ($C_7H_6O_4$; 154.12 g/mol) is a water-soluble white powder that contains a polyketide lactone structure (Saleh and Goktepe, 2019) (Figure 2.2). PAT is among the smallest polyketides. It is an alpha, beta (α, β) unsaturated compound (Hammami et al., 2017). Additionally, sulfhydryl groups (for instance, cysteine (Cys) and glutathione), free amino groups, sulphur dioxide, and ascorbic acid can interact with this electrophilic gamma (γ)-lactone (Wei et al., 2020). PAT possesses three

covalently formed cyclic adducts owing to the R-amino group's nucleophilic activity in Cys and glutamic acid residues (Pillay et al., 2015).

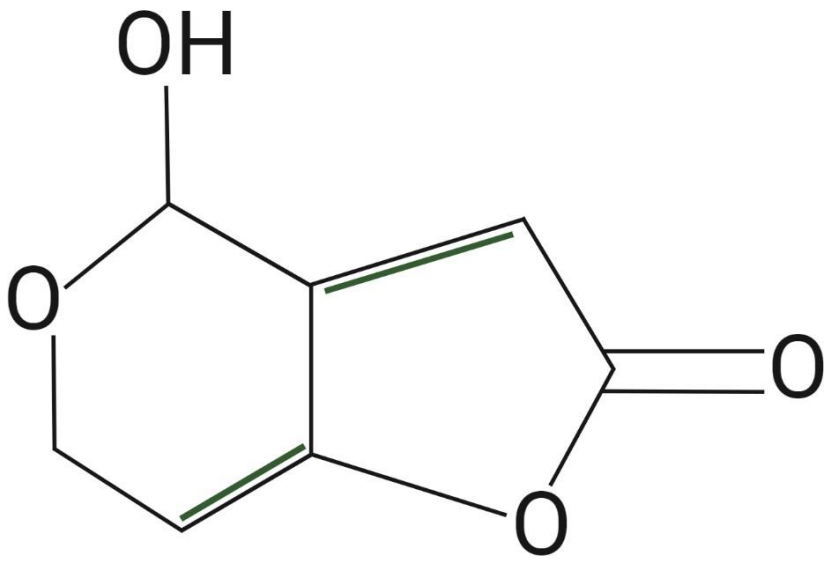

Figure 2.2: The chemical structure of PAT (4-hydroxy-4H-furo [3, 2-c] pyran-2(6H)-one; $C_7H_6O_4$) (prepared by the author using biorender.com).

2.2.4. Effects

PAT has demonstrated hepatotoxic, proteotoxic and genotoxic effects in cell cultures and animal models (Saleh and Goktepe, 2019). In animals and humans, PAT exerts gastrointestinal issues, immunotoxicity, and neurotoxicity as well as mutagenic and genotoxic effects, which result in oxidative DNA damage and cancer (Nawaf, 2023, Iqbal et al., 2024). Excessive doses of PAT may cause animal death. According to research, erythrocytes and blood-rich organs such as the liver, kidney, and spleen are primary PAT storage sites (Pillay et al., 2020). PAT damages the liver, kidneys, intestines, and immune system (Qiu et al., 2022). In a rat mycotoxicosis study by McKinley et al., purified patulin was dissolved in 0.1 mM-citrate buffer (pH 5'0) to determine concentrations: the oral, intraperitoneal, and subcutaneous doses were 4.7, 1.1, and 7.5 mg/ml, respectively (McKinley et al., 1982). Gastric intubation was used for oral administration, with an 18-gauge, 1.5-inch animal-dosing needle. The subcutaneous and intraperitoneal injections were conducted using a tuberculin syringe and 25-gauge needle (McKinley et al., 1982). The acute toxicity of a single dosage of patulin displayed consistent clinical symptoms independent of the administration route. Thus highlighting PAT's ability to induce detrimental effects regardless of the route of administration or exposure time.

PAT has been demonstrated in acute investigations to induce oedema, haemorrhages and intestinal dilatation in animal models (Pal et al., 2017). Most of the rats given PAT by the oral and subcutaneous routes that died did so within 24 hr of treatment whilst deaths were delayed in the intraperitoneal routes (25-75 hr) (McKinley et al., 1982).

Primary effects observed in subchronic investigations were hyperaemias of the duodenal epithelium and impaired renal function. Symptoms of agitation, convulsions, dyspnea, ulceration, pulmonary congestion, hyperaemia, gastrointestinal distention, and oedema were identified in all investigations (Pal et al., 2017). Cellular and animal models were used to investigate PAT's toxicity (Saleh and Goktepe, 2019).

i. PAT affects reproduction

PAT was considered teratogenic and embryotoxic to chick eggs (Awuchi et al., 2019). PAT injected into chick eggs is embryotoxic and teratogenic at 2.35-68.7 µg/egg and 1-2 µg/egg respectively (Puel et al., 2010). As an example of the effects of PAT administration in another species, a study by Guldeniz Selmanoglu investigated PAT's reproductive toxicity using Wistar albino male rats aged 5-6 weeks which were randomly assigned to four groups of ten animals each. There were two treatment groups and two control groups. All administration was done through gavage. The rats in the first treatment group (P-60) received 0.1 mg/kg bw/day of PAT for 60 days whilst the second treatment group (P-90) received 0.1 mg/kg bw/day of PAT for 90 days. The equivalent control groups (C-60 and C-90) received sterile water. The sterile water was equivalent to the amount administered to the animals in treatment groups. The dose level of 0.1 mg/kg/BW was chosen for this study. PAT was dissolved in sterile water. Selmanoglu reported that PAT had reduced sperm count while affecting sperm morphology, thus leading to a decline in male rat fertility (Selmanoğlu, 2006). Whilst an oral dosage of PAT (50 µg/day) to pregnant female Sprague Dawley rats for 1-5 days reduced litter size (Selmanoğlu, 2006). In reproduction research conducted on two-generations of male and female Sprague Dawley rats', their offspring were given 1.5 mg PAT/kg body weight/day through gavage for 7 weeks (Dailey et al., 1977). Post conception and throughout the gestational period, females were administered PAT daily. PAT increased resorption in F1 litters, but not in the F2 generation. In this generation, only a reduction in foetal weight was seen, with no evident deformations. Similar results were observed in Charles river CD-1 strain male and female mice administered 1.5 mg PAT/kg b.w. intraperitoneally; a dose of 2 mg toxin/kg b.w. aborted all embryos (Reddy et al., 1978). It is interesting to note that whilst the species, dosage and route of administration differs, resorption still occurs in Sprague Dawley rats and Charles river CD-1 strain mice at 1.5 mg PAT/kg b.w. and 2 mg toxin/kg b.w. respectively.

In female and male Swiss mice, 2 mg/PAT/kg administered daily through gastric intubation caused mortality due to brain, lung, and skin haemorrhages (Osswald et al., 1976).

The studies have observed ways in which PAT is embryotoxic and teratogenic even leading to mortality. This highlights that regardless of the species, gender or route of administration, PAT affects reproduction in various ways.

ii. Neurotoxic effects

Rat models exhibited neurotoxicity after recurrent dosages of PAT (Awuchi et al., 2019). Certain herds of beef cattle experienced severe neurotoxicity upon exposure to *Aspergillus clavatus* and PAT in their diet (Pal et al., 2017). Animal necropsies revealed the degeneration of neurons and axons in the CNS and PNS, respectively. Additionally, lesions in the nerves were observed. PAT seems to target the neurons and nerves which are fundamental to communication pathways, thus resulting in neurotoxic effects or neural abnormalities. PAT depletes ATP in neuro-2a cells, leading to dysfunctional mitochondria and lysosomes (Pal et al., 2017).

iii. Immunological effects

Additional sources of PAT, including fruits, juices, and jams, have been demonstrated *in vitro* to reduce immune system responses (Kraft et al., 2021). PAT inhibits interferon-producing T-helper type 1 cells (Pal et al., 2017). PAT therapy significantly reduced Lipopolysaccharide (LPS)-induced transcription of pro-inflammatory TNF-α and IL-6 genes in a dose-dependent manner. Overall, PAT inhibits pro-inflammatory cytokine production in LPS-induced macrophages (Hong et al., 2023). It also has immunosuppressive properties (Moss, 2008). PAT may target pro-inflammatory cytokines to reduce the body's immune response. PAT-exposed animals have exhibited impaired immunity. The findings of these animal studies indicate that humans are equally susceptible to immune system disturbances caused by PAT (Awuchi et al., 2019).

iv. Carcinogenic effects

PAT was classified as a Group 3 agent by the International Agency for Research on Cancer (IARC), as it may be carcinogenic; however, there is inadequate data to establish this (Chu et al., 2021). In 1982, a considerable rise in hyperplastic nodules in F344 male rat livers was noted after introducing PAT (4 ppm) to their diets during a six-week study. Thus indicating the ability of PAT to be

tumorigenic in the liver (Saleh and Goktepe, 2019). Birth abnormalities and cancer can result due to the presence of PAT in the decaying apples and pears utilised by juice companies in recent years (Nawaf, 2023). PAT may induce colorectal cancer and fibroadenomas (Nawaf, 2023). The main source of PAT-induced skin cancer is contact with decomposing fruits. In PAT-induced skin carcinoma, apoptosis is disrupted as the phosphorylation of B-cell lymphoma 2 (BCL 2)-associated agonist of cell death (BAD) is inhibited (Nawaf, 2023). Research has found that applying Patulin (400 nM) to the skin of female Swiss albino mice enhanced the production of ROS, doubled cellular proliferation, and resulted in tumour growth within two weeks (Saleh and Goktepe, 2019). Utilising oxidative stress and apoptosis is a plausible mechanism of action for PAT-induced carcinogenicity.

i. **Disruption of biological processes**

PAT disrupts a cell's plasma membrane (Pal et al., 2017). Additionally, PAT impedes the following processes, sodium (Na+)-coupled amino acid transport, transcription and translation, DNA and protein synthesis (Pal et al., 2017). PAT's inhibitory influence on several enzymes (RNA polymerase, lysosomal enzymes, ATPase) is well attributed to its relationship with sulfhydryl groups (Saleh and Goktepe, 2019). PAT impairs mitochondrial integrity and ATP generation (Pillay et al., 2020). By disrupting several enzymes, affecting the mitochondria and its affinity for sulfhydryl groups, it strengthens oxidative stress as PAT's mechanism of action. By influencing ion transport, disrupting enzyme activity, and impeding amino acid intake and protein production, PAT induces cytotoxicity (Frizzell et al., 2014).

ii. **Proteotoxic effects**

PAT exerts a profound influence on the generation of vital proteins involved in cell junctions, membrane potential, gene expression, protein production, and cell signalling (Ramalingam et al., 2019). PAT may be proteotoxic. Studies suggest that proteotoxic molecules typically have sex-dependent responses (Guerra-Moreno and Hanna, 2017). Research indicates that males are more vulnerable than females to the deleterious effects of mycotoxins, which are frequently neglected in toxicological investigations (Saleh and Goktepe, 2019). In 2018, Soler et al. found that PAT alters endocrine function. To accurately evaluate results in hormonal research, both male and female models should be employed (Soler and Oswald, 2018). Administering PAT (0.1 mg/kg/day) affects the thyroid at histopathological and hormonal levels in developing male rats (Selmanoğlu, 2006). PAT interacts with proteins comprising histidine or lysine and reduces Cys levels (Saleh and Goktepe, 2019). Inter and intra-molecular protein cross-linking were induced by PAT. Covalent adducts are formed when PAT reacts with electrophilic chemicals (Saleh

and Goktepe, 2019). PAT has strong reactivity with cellular nucleophiles and the ability to react quickly with sulfhydryl groups but gradually with amino functionalities in proteins, and glutathione accounts for its genotoxic and cytotoxic effects (Glaser and Stopper, 2012). The ability to inhibit enzymes is attributed to PAT's preference for compounds possessing sulfhydryl groups (SH) such as cysteine (Cys) and glutathione, thus aiding in its deleterious effects (Frizzell et al., 2014, Awuchi et al., 2019). This links tos PAT's ability to disrupt biological processes in the aforementioned section. PAT-induced cytotoxicity is mediated by its ability to diminish cellular glutathione levels (Frizzell et al., 2014). The protein cross-linking is achieved through a preferential reaction with Cys' thiol group; however, it can occur with the side chains of histidine, lysine, and the α-amino group (Pal et al., 2017). The proteasome is modulated by the regulatory particle non-ATPase 4 (Rpn4) transcription factor, which breaks down proteins (Saleh and Goktepe, 2019). PAT overexpresses the Rpn4 gene by activating the Rpn4 transcription factor. The overexpression of Rpn4 is proteotoxic and degrades proteins (Saleh and Goktepe, 2019).

iii. **PAT exerts nephrotoxic effects**

In human embryonic kidney (HEK293) cells, PAT inhibits proliferation, possibly by elevating oxidative stress levels, which results in apoptosis (Zhang et al., 2015). PAT damages DNA in HEK293 cells (Zhang et al., 2015). PAT affects HEK293 cells by inducing apoptosis through oxidative stress and DNA damage, thus affecting the cell line and possibly is a mechanism of action in the kidney. In rat kidney tissues, PAT leads to apical microvilli, mitochondria, and the convoluted tubules' brush border loss, in addition to an interstitial inflammatory cell influx (Ramalingam et al., 2019).

iv. **PAT-induced hepatotoxicity**

The intraperitoneal injection of PAT increased serum levels of liver function biochemical markers, alkaline phosphatase (ALP), aspartate aminotransferase (AST), and alanine aminotransferase (ALT) in Kunming, BALB/c, and C57BL/6 mice (Wei et al., 2020). Intraperitoneally injecting PAT (2mg/kg) in Swiss albino male mice increases lipid peroxidation, malondialdehyde (MDA) generation, and protein carbonyl levels in the liver while decreasing antioxidant activity, particularly superoxide dismutase (SOD), catalase (CAT), glutathione (GSH), glutathione peroxidase (GPx) and glutathione reductase (GR) (Jayashree et al., 2017). An increase in the loss of mitochondrial membrane potential and reactive oxygen species (ROS) levels along with a reduction in the activation of serine (Ser)/threonine (Thr) kinase 1 (AKT 1) and mammalian target of rapamycin (mTOR) was observed in a PAT-administered (0-2μM) HepG2 cell model (Wei et al., 2020). At similar doses, PAT is able to induce oxidative stress in different

models. PAT activated the p53 and mitogen-activated protein kinase (MAPK) pathways to induce liver damage in intraperitoneally injected BALB/c mice (Wei et al., 2020). PAT ingestion causes serious histopathologic harm in mice livers (Wei et al., 2020). Liver hypertrophy, inflammation, and cellular necrosis were observed in male albino mice upon oral treatment of PAT (0.1 mg/kg/ b.w.) (Wei et al., 2020). An experiment by Jayashree et al. revealed that an oral dosage of PAT (2 mg/kg/b.w.) caused serious histopathologic alterations in male BALB/c mice, including localised hepatocellular vacuolation and mild haemorrhages (Jayashree et al., 2017). At an oral dose of 0.1 and 2 mg/kg/b.w. PAT induces histological changes. In primary hepatocytes preparations, PAT-mediated effects varied significantly among 3 different individuals (n=3). In one case, exposure to 50 mM (7706 ng/ml) only resulted in a 20% reduction in cell viability, while in others, a 5 mM (770.6 ng/ml) dosage further reduced cell viability significantly (Frizzell et al., 2014). The difference in cell viability could be attributed to two variables: the individual or the concentration administered. The observed 20% reduction in the first hepatocyte samples possibly had better integrity and thus was able to repair or protect itself against any PAT-mediated effects as opposed to the other samples.

Research gaps

Studies have focused on the effects of PAT in the body, including the kidney, nervous system and immune system, amongst others. However, research on PAT in the liver is sparse, including mechanistic studies. Research is required on the effect that PAT has in the liver's MAPK/ERK/PI3K/AKT pathways, additionally on the liver-specific adrenergic receptors that regulate the above-mentioned pathways. There is limited research on PAT's influence on DNA methylation in the liver.

2.3. The liver

The liver possesses remarkable regenerative capabilities (Tao et al., 2022). Even vertebrates have a great capacity for liver regeneration, making the liver a unique organ. Through hepatocyte proliferation and differentiation, the liver can regenerate up to 70% of its bulk (Wen et al., 2022). Dormant hepatocytes can return to the cell cycle and divide to regain tissue equilibrium after acute damage or partial hepatectomy (Tao et al., 2022). Using enterohepatic circulation, the liver is the initial organ to receive PAT from the intestines (Wei et al., 2020). PAT disrupts the intestinal barrier, enabling easier passage from the intestinal lumen to the portal blood supply. PAT targets the liver, an organ responsible for the biotransformation of substances and blood detoxification (Wei et al., 2020).

2.3. Adrenergic receptors

Adrenergic receptors (ARs) are members of the G protein-coupled receptors (GPCRs) that bind to norepinephrine and epinephrine and activate the sympathetic nervous system (SNS) (Chen et al., 2020). Liver damage, fibrosis and regeneration are SNS-regulated (Chen et al., 2020). They have three intracellular, extracellular, and seven exceptionally preserved hydrophobic transmembrane regions. These domains stretch across the lipid bilayer. Additionally, all adrenoreceptors are attached to a GTP-binding protein (Strosberg, 1993). Their polypeptide chain ranges between 400 and over 500 residues, with various amino and carboxy-terminal sections (Strosberg, 1993). ARs regulate tissue homeostasis and have been linked to several illnesses (Chen et al., 2020). The adrenergic receptors possess three categories: alpha-1 (α1-AR), alpha-2 (α2-AR), and beta (β-AR). Depending on their pharmaceutical attributes, these categories are sub-categorised into: α-1A, α- 1B, α-1D; α-2A, α-2B, α-2C; β-1, β-2, and β-3 (Pillay et al., 2020). Based on the tissue location, the adrenoreceptor subtypes may exhibit varied effects, despite belonging to the same main type (Wu et al., 2021). Adrenergic receptors modulate liver repair, tissue equilibrium, innate immunity, and fibrosis (Chen et al., 2020). A healthy liver contains two major ARs: α-1 and β-2 ARs. In healthy livers, α-1A is the most prevalent a1-AR subtype (Chen et al., 2020). Rodent and human livers possess β1- and β2-ARs (Ghosh et al., 2012). Hepatic stellate cells express α1-AR, α2-AR, β1-AR, and β2-AR (Schwinghammer et al., 2020). Kupffer cells, hepatocytes, and extrahepatic endothelial cells have all been shown to express α2-AR (Schwinghammer et al., 2020). Liver damage or fibrosis alters the adrenergic receptors (Schwinghammer et al., 2020). In vivo studies demonstrate that liver fibrosis exclusively affects α1-AR and β-AR (Schwinghammer et al., 2020). Injuries or partial hepatectomy induces hepatic α1-AR-regulated hepatocyte proliferation, regeneration, and metabolic function (Han et al., 2008). The α2A-AR receptors reduce blood pressure and sympathetic output (Philipp et al., 2002). The α2A-AR in sympathetic nerves appears to regulate norepinephrine release during periods of maximum sympathetic activation. After a liver injury, α2B-AR levels increase (Schwinghammer et al., 2020). Liver cirrhosis and portal hypertension patients had reduced α1-AR levels, but individuals with cirrhosis and a CCl4 fibrosis model had much higher levels of β3-AR. In non-alcoholic fatty liver disease (NAFLD), during early fibrosis, α1, β1, β2, and β3-AR levels are lowered, but with increasing fibrosis/cirrhosis, they are substantially elevated (Schwinghammer et al., 2020).

β-adrenergic receptors exist in various organs, including hepatocytes, kidneys, the central nervous system, adipocytes, lymphocytes, endothelial cells, and bronchial and vascular smooth muscle cells (Vasudevan et al., 2011). The β-ARs principally regulate cellular function. The ability of β- AR to perceive and send signals into cells determines its functional status (Vasudevan et al., 2011). The β1-AR is the most prevalent subtype in the heart (Giltrow et al., 2011). A study by Zapater et al. revealed that in CCl_4-treated mice with bacterial DNA, hepatic norepinephrine modulates the pro-inflammatory response through β1-AR (Zapater et al., 2012). Over-expression of β1-adrenergic receptors may cause liver damage, according to growing research (Wu et al., 2022). Signalling responses to environmental stimuli and ligands are regulated by the archetypal GPCRs, β2-AR (Tao et al., 2022). Furthermore, β2-AR regulates liver regeneration mechanisms including growth factors, cytokines, and metabolic systems (Tao et al., 2022). Pathophysiological diseases, notably cancer, occur due to abnormal β2-AR expression (Tao et al., 2022). Levels of β2-AR are higher in regenerated liver cells. Studies have revealed an increase in β2-AR levels during 70% partial hepatectomy-induced liver regeneration (Tao et al., 2022). Two days after partial hepatectomy, deleting β2-AR in mice resulted in a 62% mortality rate, lower proliferation markers, and poor liver function in regeneration. In β2-AR-deficient livers, after partial hepatectomy, and in hepatocytes post hepatocyte growth factor therapy, the mitogen-activated protein kinase/extracellular signal-regulated kinase (MAPK/ERK) pathway which regulates cellular proliferation, was substantially impaired (Tao et al., 2022). Research has found that during liver regeneration, β2-AR deletion disrupts the MAPK/ERK pathway (Tao et al., 2022). β3-ARs are primarily located in adipocytes (Trebicka et al., 2009). This receptor which promotes adipose tissue (brown and white) thermogenesis and lipolysis, was not found in human or rat liver (Ghosh et al., 2012).

2.3.1. Adrenergic receptor signalling

The α1-AR modulates cellular processes through diverse secondary messengers (Pillay et al., 2020). The α1-AR regulates the function of different effectors, comprising MAPKs and phosphatidylinositide 3-kinase (PI3K). Triggering α1-AR activates MAPK/ERK and phosphatidylinositol-3-kinase/protein kinase B and alpha Ser/Thr protein kinase PI3K/PKB (also known as PI3K/AKT) pathways (Mazibuko et al., 2024).

To interact with the Gq/protein family, α1-AR is activated and structurally modified (Figure 2.3). This ensures phospholipase C (PLC) is stimulated, which transforms phosphatidylinositol-1, 2-bisphosphate (PIP_2) to inositol triphosphate (IP3) and diacylglycerol (DAG), thus liberating intracellular calcium (Ca^{2+})(Pillay et al., 2020). DAG and Ca^{2+} induce smooth muscle contractions and stimulate protein kinase C (PKC), which phosphorylates proteins and regulates the process. This includes MAPK, PI3K, and p21-rat sarcoma (ras) (Pillay et al., 2020). The MAPK family, which includes the ERK, Jun N-terminal kinase (JNK), and p38 kinases, coordinate α1-AR- regulated growth responses. The α-AR stimulate the MAPK/ERK and PI3K/AKT signalling pathways, which promote their physiological activities (Mazibuko et al., 2024).

Research indicates that activated β-AR promotes mitogen-activated protein kinase (MAPK) signalling pathways (Vasudevan et al., 2011).

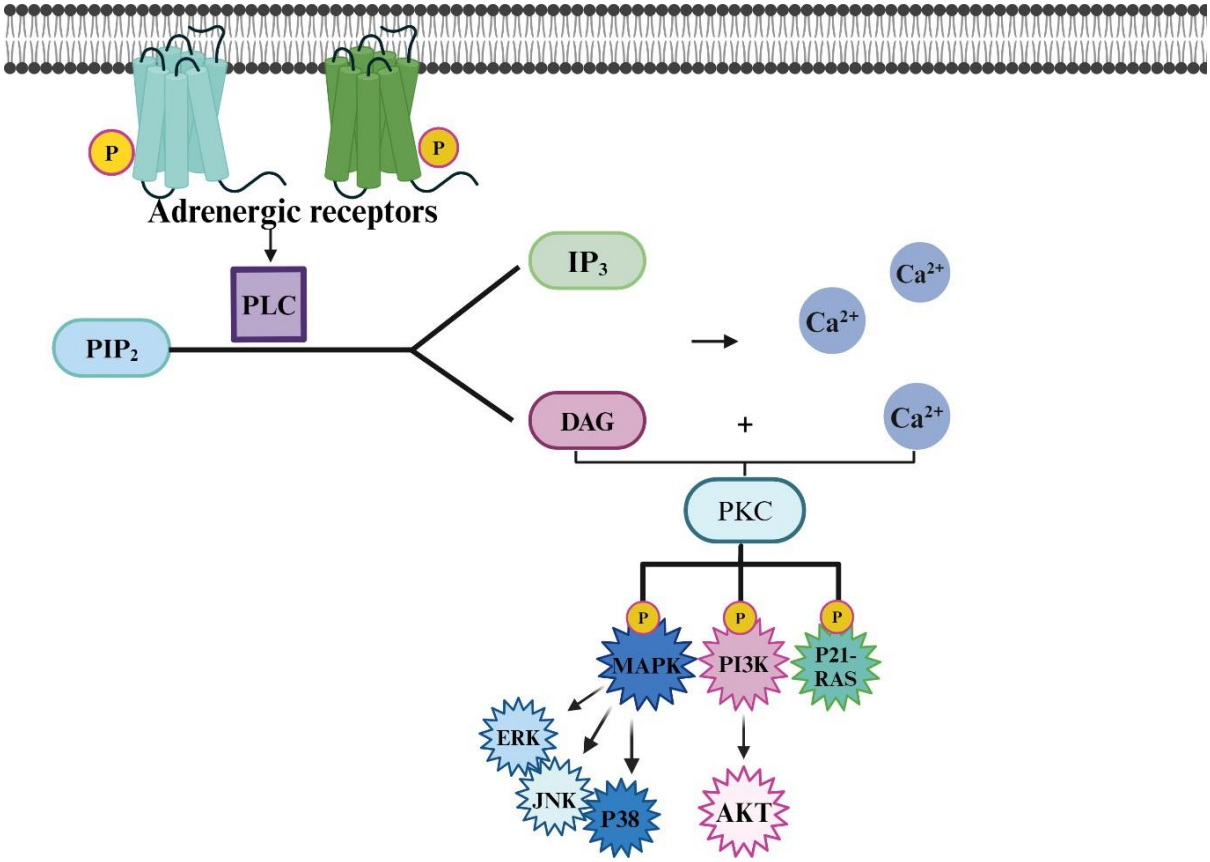

Figure 2.3: The adrenergic receptor signalling pathway (prepared by author using biorender.com)

2.3.2. The MAPK/ERK pathway

Phosphorylation processes that phosphorylate MAPK-regulated transcription factors and cytosolic proteins modulate MAPK functions (Pillay et al., 2020). MAPKs are classified into several types, most notably ERK1/2. The GPCRs and receptor tyrosine kinases (RTKs) initiate the ERK signalling pathway. A signal is transmitted to the protein kinases rapidly accelerated fibrosarcoma (Raf)-1, A-Raf and B-Raf (Rafs) after these receptors stimulate Ras with GTP (Mazibuko et al., 2024). Activated Raf protein stimulates MEK1/2 (MAPK/ERK kinase or MAP kinase kinase), which activates ERK1/2 by phosphorylation and consequently modulates mitosis, differentiation, gene expression, cellular metabolism and apoptosis (Mazibuko et al., 2024). The p21 and Ras Gq/mediated interactions as well as direct stimulation by PKC and Ca^{2+} may trigger the ERK 1/2

pathway. This action may assist in α1-AR-mediated DNA generation and cell proliferation (Pillay et al., 2020). PI3K transforms phosphatidylinositol (4, 5)-bisphosphate **(**PIP_2) to phosphatidylinositol (3, 4, 5)-phosphate (PIP_3) by working downstream of Ras. This causes AKT/PKB (protein kinase B) to localise to the membrane and be phosphorylated (Pillay et al., 2020). Proteins and transcription factors governing cell metabolism and survival are phosphorylated by activated AKT. Inhibiting AKT leads to malfunctioning mitochondria-induced cell death (Pillay et al., 2020). The redox-sensitive MAPK and AKT signalling pathways are essential for cellular function and longevity. The MAPK family's proline-directed Ser/Thr protein kinases are prototyped by ERK1 and ERK2 (Wen et al., 2022). In mice livers, ERK encourages hepatocyte proliferation and differentiation (Wen et al., 2022).

The ARs trigger the ERK pathway through β-arrestins and G-protein-dependent processes. Constituents of the MAPK pathway are recruited by β-arrestins to endosome membranes, which activates ERK (Mazibuko et al., 2024). The β-arrestins then impede the migration of active ERK to the nucleus, which promotes the ERK signalling cascade. The MAPK/ERK and PI3K/AKT pathways impact cytoskeletal organisation, cell growth, proliferation, metabolism, longevity, and cell death (Mazibuko et al., 2024) (Figure 2.4).

2.3.3. The PI3K/AKT pathway

During stress, the PI3K/AKT pathway impacts cell survival. The lipid kinase PI3K phosphorylates inositol phospholipids in the 3'OH group. AKT/PKB promotes various cell activities, notably cell cycle progression and survival (Mazibuko et al., 2024).

The reaction between growth factors and RTKs stimulates the PI3K/AKT signalling cascade (Shamsan et al., 2024) (Figure 2.3). Based on its substrates and configurations, PI3K is divided into three categories. Their regulatory and catalytic subunits bind to phosphorylated tyrosine residues on active RTKs, particularly the p85 subunit. Stimulants of PI3K include ligand-activated receptors, cytokines, hormones, and growth factors, this results in the formation of a protein complex (Src homology and Collagen/Growth Factor Receptor-bound protein 2/ Son of sevenless proteins) (Shc/GRB2/SOS) that activates Ras (Mazibuko et al., 2024). Active Ras initiates p110 and PI3K. PIP_2 is then phosphorylated, yielding PIP_3 (Shamsan et al., 2024). To convert PIP_2 to PIP_3, the α1-AR uses a Gq α-subunit and PTx-insensitive G proteins. PIP_3 engages and enhances

AKT activation by phosphoinositol-dependent kinase-1 (PDK1) and AKT on threonine 308 (Thr308) pleckstrin homology (PH) site in the kinase domain (T-loop) (Wang et al., 2017) (Figure 2.4). AKT's Ser473 residue is phosphorylated by PDK2 (mammalian target of rapamycin complex 2 (mTORC2)), thus fully activating it and initiating its cascade. Activated AKT enhances growth, DNA repair and survival and phosphorylates transcription factors and proteins including BAD, murine double minute 2 (MDM2), glycogen synthase kinase-3 beta (GSK3β) and mTOR thus suppressing apoptosis (Mazibuko et al., 2024). Hindering AKT induces mitochondrial malfunction resulting in apoptosis (Pillay et al., 2020).

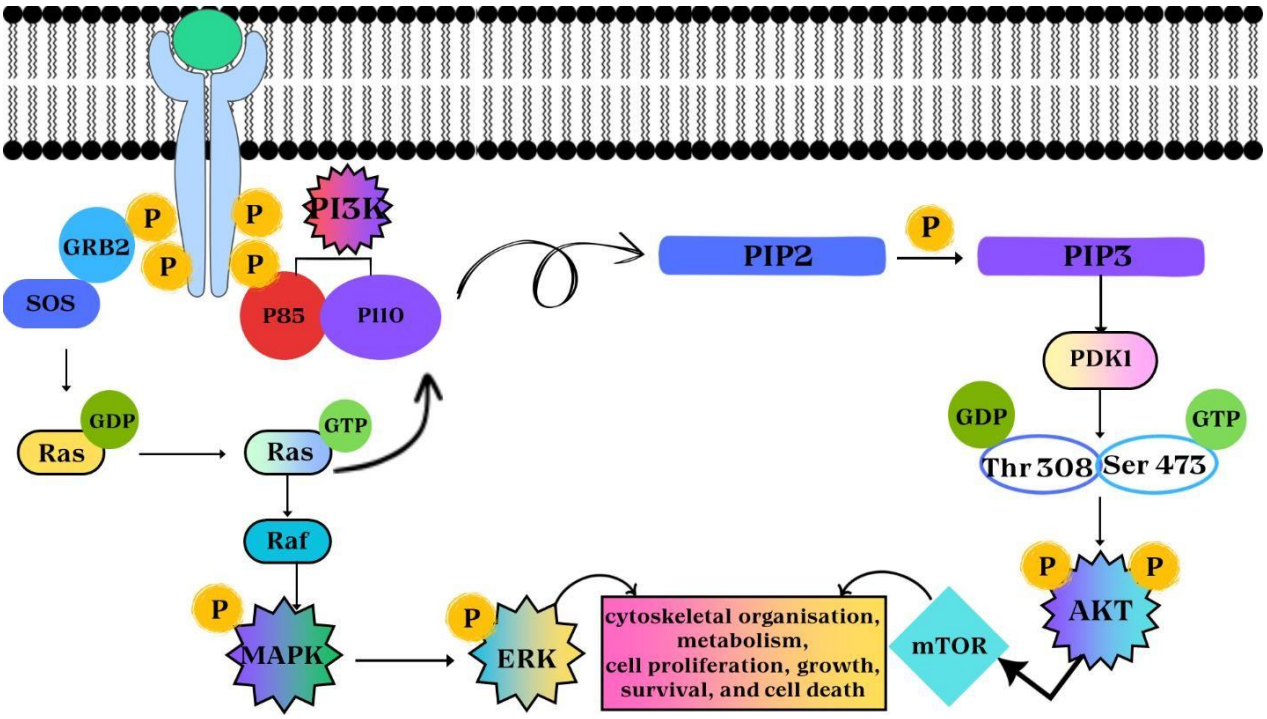

Figure 2.4: The MAPK/ERK and PI3K/AKT signalling pathways (prepared by author using canva.com)

2.4. Epigenetics

Epigenetics is mitotic and meiotic hereditary alterations in gene expression due to chemical modifications to DNA, non-coding RNAs and histones, without affecting the DNA sequence (Menezo et al., 2016, García-Guede et al., 2020). Epigenetic mechanisms consist of histone modifications, microRNAs and DNA methylation. The focus of this study is DNA methylation as it is a common epigenetic mechanism. Gene expression is either stimulated or inhibited as these

alterations remodel the chromatin. Eukaryotic organisms require gene silencing at the chromatin level to function properly (García-Guede et al., 2020). DNA methylation is a widely researched and well-known epigenetic process. Microbial cells, animals and plants require DNA methylation for normal growth and differentiation (Bind et al., 2022). DNA methylation is a natural procedure which suppresses chromatin structure, promotes genomic stability, silences genes and regulates pluripotency genes, oncogenes, transposons, genomic imprinting, and X-chromosome deactivation (Ghazi et al., 2020). DNA methylation regulates gene expression (Bind et al., 2022). During cell proliferation, development, and differentiation, DNA methylation regulates gene silencing at the transcriptional level. Additionally, in adult organisms, it creates distinctive cell lineages (Ghazi et al., 2020).

Eukaryotic DNA methylation primarily happens when the universal methylation cofactor S-adenosylmethionine (SAM) donates a methyl group (CH_3) that is added to cytosine's 5th carbon at 5'-Cytosine-phosphate-Guanine-3' (CpG) dinucleotides yielding 5-methylcytosine (5-mC) (Ghazi et al., 2020) (Figure 2.5). When CH_3 is donated, SAM is transformed to S-adenosylhomoCys (SAH), which is then hydrolysed by adenosylhomocysteinase hydrolase (Ahcy) back to homoCys (Hcy). Ahcy will prioritise SAH production over hydrolysis if Hcy cannot be metabolised by the transsulfuration pathway or re-methylated to methionine (Ghazi et al., 2020). DNA methylation and DNMT activity are hindered by excess SAH levels. DNMTs catalyse DNA methylation (García-Guede et al., 2020). DNMT1 prefers hemimethylated substrates and maintains methylation patterns post-DNA replication (Bönsch et al., 2006, García-Guede et al., 2020). Methylation patterns are set when the *de novo* methyltransferases DNMT3A and DNMT3B induce DNA methylation in non-methylated cytosine bases (Ghazi et al., 2020).

Demethylation can occur by removing the methyl group from 5-mC and eliminating substances produced by DNA repair, or by directly removing 5-mC following conversion to thymine and excision repair (Menezo et al., 2016). Whilst DNA methylation is very stable, the CH_3 group must be removed passively, actively or using both processes for epigenetic regulation (Bind et al., 2022). Passive DNA methylation which happens during replication cycles, requires freshly synthesised DNA strands (Bind et al., 2022). Active demethylation processes are facilitated by methyl-CpG-binding domains (MBDs) (Menezo et al., 2016) (Figure 2.5).

Abnormal DNA demethylation results due to uncontrolled 5-HmC levels (Menezo et al., 2016). Chromatin structure and gene expression are altered if heritable DNA methylation patterns are disrupted (Bönsch et al., 2006). Dysregulated DNA methylation can cause diseases such as cancer (García-Guede et al., 2020).

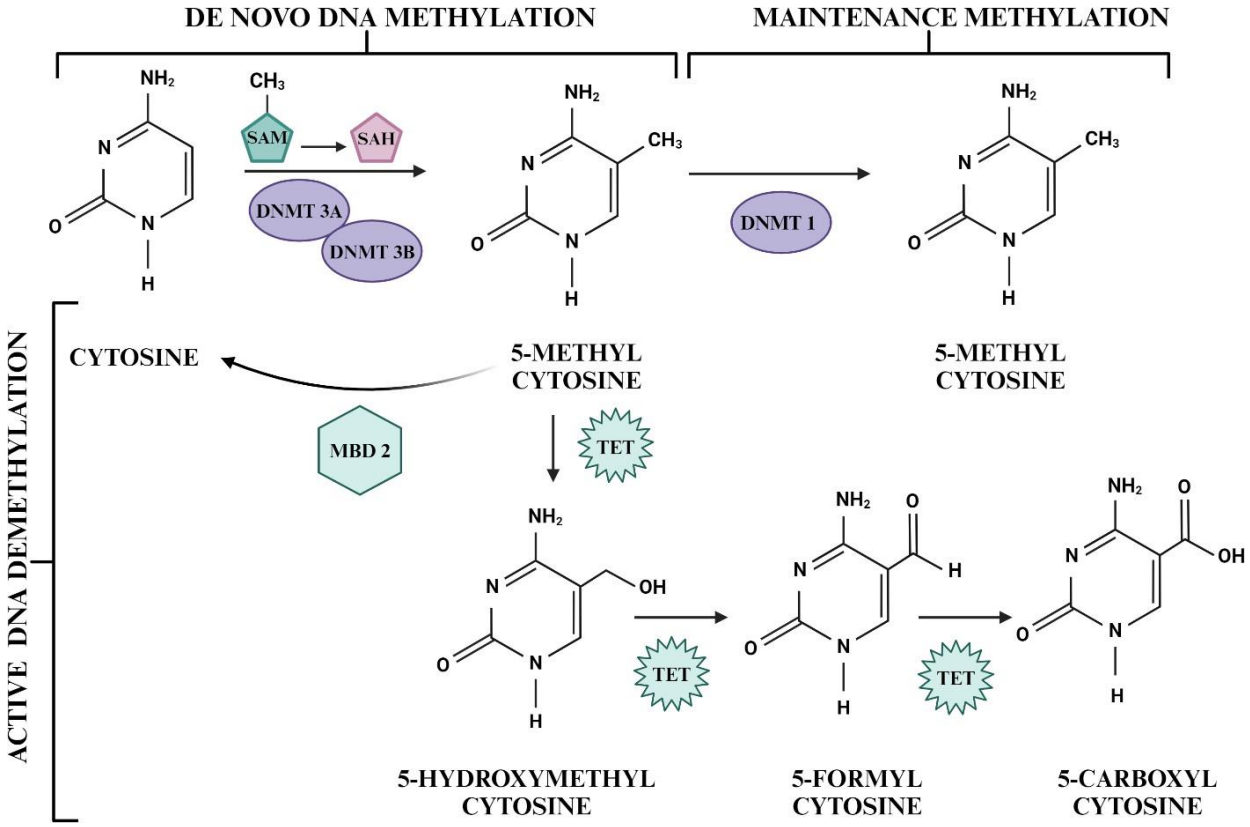

Figure 2.5: DNA methylation and demethylation processes (prepared by the author using biorender.com)

Chapter 3: Materials and Methods

3.1. Materials

PAT (P1639) was acquired from Sigma-Aldrich (Missouri, USA). Primer sequences were purchased from Inqaba Biotechnical Industries (Pty) Ltd (Pretoria, South Africa). The apparatus and reagents for western blotting were purchased from Bio-Rad (Hercules, CA, USA). Abcam (Cambridge, UK), Cell Signalling Technology (Danvers, Massachusetts, USA), Proteintech (Sankt Leon-Rot, Germany), Santa Cruz Biotechnology (Dallas, Texas, USA), and Sigma Aldrich (Missouri, USA), supplied the antibodies. The DNA Methylation Quantification Kit was acquired from Abcam (Cambridge, UK). Unless otherwise noted, all reagents were procured from Merck (Darmstadt, Germany).

3.2. Animal Ethics and Procedure

All procedures complied with the norms and regulations established by the University of KwaZulu-Natal Animal Research Ethics Committee and the Animal Research: reporting of *in vivo* experiments (ARRIVE) standards (Appendix A). The investigation took place at the Howard College Campus of the University of KwaZulu-Natal, involving eight male C57BL/6 mice. Mice were kept at the Africa Health Research Institute (AHRI) of the University of KwaZulu-Natal, Nelson R. Mandela Medical School, Durban, South Africa, under conventional aseptic settings (temperature: 25ºC, humidity: 40-60%, 12-hour (hr) light and dark cycles).

3.3. Tissue preparation

Eight mice, approximately six to eight weeks old, were randomly categorised into control and PAT-fed groups (n=4). To validate my sample size, mice studies by (Schütze et al., 2010, Mulder et al., 2015) utilised a sample size of n=4. For a small sample size, ≤15 values per group are required for a t-test (Mishra et al., 2019).

The control group were administered 0.1 M phosphate-buffered saline (PBS). The PAT group was administered 2.5 mg/kg of PAT orally at 0.250 ml/23g on day zero and then daily for ten days (Jin et al., 2016, Mazibuko et al., 2024).

PBS (0.1 M) was used to prepare PAT. Post the ten-day treatment, four mice from each group were sacrificed. Subsequently, the livers were collected, homogenised, and kept at -80°C in Cytobuster™

Protein Extraction Reagent (Novagen, 71009) and Qiazol reagent (Qiagen, 79306) for protein and RNA extraction, respectively.

3.4. Quantitative PCR assay

3.4.1. Quantitative PCR introduction

Quantitative PCR (qPCR) recognises and quantifies gene expression (Kralik and Ricchi, 2017, Freitas et al., 2019). This assay encompasses RNA isolation and cDNA synthesis. An RNA sample is converted into complementary DNA (cDNA) through reverse transcription. Primers and SYBR green are then used, with SYBR green intercalating between the bases of the newly formed double- stranded DNA (Wilhelm and Pingoud, 2003, Antônio José et al., 2016). After each cycle, fluorescence is quantified (Kralik and Ricchi, 2017). There is a direct relationship between the fluorescence and the quantity of PCR product generated (Antônio José et al., 2016). Increased DNA production leads to greater fluorescence detection in qPCR reactions (Adams, 2020). A reference gene particularly glyceraldehyde-3-phosphate dehydrogenase (GAPDH) is employed to normalise the target gene (Antônio José et al., 2016). This assay can evaluate mRNA levels (Antônio José et al., 2016). The mRNA expression of *alpha (α1, 2A and 2B) and beta (β-1, 2, 3) adrenergic receptors, PI3K, AKT, MAPK, MAPK14, ERK1/2, DNMT1, DNMT3A and DNMT3B, and MBD2* were probed for using qPCR.

3.5. RNA isolation

The mice livers were homogenised in a microcentrifuge tube containing 500 µl of Qiazol reagent. All samples were administered with 100 µl of chloroform and incubated at room temperature (RT) for 2-3 minutes (min). The microcentrifuge tubes were centrifuged (4°C, 12,000 xg, 15 min). The supernatants were pipetted into new microcentrifuge tubes and to each sample 250 µl of isopropanol was added. After vortexing, the samples were incubated overnight (-80°C). The samples were centrifuged (4°C, 12,000 xg, 20 min). After discarding the supernatant, the pellet was rinsed with 500 µl of 75% cold ethanol and centrifuged (4°C, 7400 xg, 15 min). The ethanol was discarded. The pellet was air-dried until it was transparent (2 hr). The pellet was re-suspended in 30 µl of nuclease-free water, incubated (RT, 2-3 min), vortexed and stored (-80°C).

3.5.1. RNA quantification

The Nano-drop 2000 spectrophotometer (ThermoFisher Scientific) quantified the RNA samples. All samples were standardised to 1000 ng/µl. The A260/A280 absorbance ratio evaluated the RNA purity. At a ratio of 2.0, RNA was considered pure.

3.5.2. Complementary DNA (cDNA) synthesis

Utilising the Maxima H minus first strand cDNA synthesis kit (ThermoFisher Scientific, K1652), cDNA was generated (Table 3.1).

Table 3.1: Master Mix 1 recipe using the Maxima H minus first strand cDNA synthesis kit (ThermoFisher Scientific, K1652)

Reagent	Volume per reaction
Oligo deoxythymidine (dT) 18 primer (18 pmol)	0. 25 µl
10 mM Nucleoside triphosphate (dNTP) mix	1. 00 µl
Nuclease free water	12.75 µl

In micro-centrifuge tubes, 14 µl of master mix 1 and 1 µl of template RNA were added. The contents were mixed gently and incubated in a thermocycler (65°C, 5 min). Thereafter samples were left to chill on ice. Into the aforementioned micro-centrifuge tubes, 5 µl of master mix 2 was added to all samples and mixed gently (Table 3.2).

Table 3.2: Master Mix 2 recipe using the Maxima H minus first strand cDNA synthesis kit (ThermoFisher Scientific, K1652)

Reagent	Volume per reaction
5x Reverse transcriptase buffer	4 µl
Maxima H minus enzyme mix	1 µl

The samples were then placed in the thermocycler, where they underwent incubation (65°C for 10 min followed by 50°C for 15 min and 85°C for 5 min). Following these time frames, 60 µl of nuclease-free water was introduced to each sample and stored (-80°C).

3.5. Polymerase chain reaction

The inexpensive and time-saving technique, polymerase chain reaction (PCR) amplifies particular DNA sequences from template strands using primers that extend the target gene. PCR is made up of three primary steps (Delidow et al., 1993, Hays et al., 2024) (Figure 3.1):

1) **Denaturation (90°C)**

The double-stranded DNA template is denatured into single strands.

2) Annealing (55°C-60°C)

Primers are annealed to each original strand for new strand synthesis from the 3’ ends.

3) Extension (72°C)

Thermus aquaticus (Taq) DNA polymerase adds deoxynucleotide triphosphates (dNTPs) to the 3' end of the primers to extend a new double-stranded DNA.

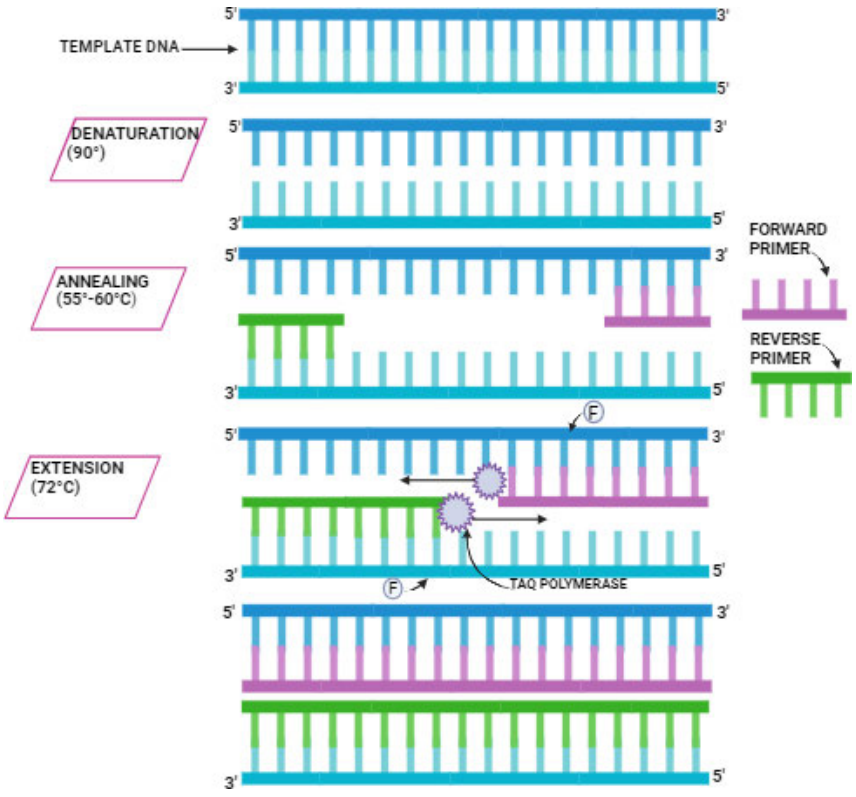

Figure 3.1: The principle of the PCR assay (prepared by author using biorender.com).

3.6. Quantitative PCR Protocol

Original primer stocks are 100 µM. Primer stocks (25 µM) were prepared using 25 µl of primer and 75 µl of nuclease-free water. A master mix was made up of the following reagents and volumes (Table 3.3):

Table 3.3: The qPCR Master mix recipe

Reagent	Volume per reaction
SYBR Green (Thermo Fisher Scientific, A25742)	5 µl
Nuclease-free water (Ambion®, AM9906)	2 µl
Sense primer (25 µM)	1 µl
Anti-sense primer (25 µM)	1 µl

To a 96-well plate, 9 µl of the above master mix and 1 µl of cDNA were pipetted in triplicate. The plate was sealed using an adhesive plate seal and centrifuged (24°C, 10 000 xg, 1 min). The plate was placed in the QuantStudio™ 3 Real-Time PCR instrument (ThermoFisher Scientific, A28132) at the following conditions:

The hold stage

Step 1: Initial denaturation (95°C, 10 min)

The PCR stages (for 40 cycles)

Step 1: Denaturation (95°C, 15 seconds)

Step 2: Annealing (65°C, 40 seconds) - specific temperatures for each primer in Table 3.4 Step

3: Extension (72°C, 30 seconds)

The melt curve stages

Step 1: 95°C, 15 seconds

Step 2: 60°C, 1 min

Step 3: 95°C, 1 second (Dissociation)

The results were analysed using the QuantStudio™ Design and Analysis Software version 1.5.1. (ThermoFisher Scientific, Waltham, MA, USA). The mRNA expression fold changes were evaluated employing the comparative threshold cycle (Ct) method.

Table 3.4: The qPCR annealing temperatures and primer sequences purchased from Inqaba Biotechnical Industries (Pty) Ltd.

Gene	Annealing temperatures (°C)	Primer Sequence (5'- 3')
Alpha-adrenergic receptor 1A (α1A-AR)	54.7°C	F: CGGTGACTCACTACTACATTGTC R: GACGCTGTGCAGCATAAGAC
Alpha-adrenergic receptor 2A (α2A-AR)	57°C	F: GTGACACTGACGCTGGTTTG R: CCAGTAACCCATAACCTCGTTG
Alpha-adrenergic receptor 2B (α2B-AR)	57°C	F: TCTTCACCATTTTCGGCAATGC R: AGAGTAGCCACTAGGATGTCG
Beta-adrenergic receptor 1 (β1-AR)	62°C	F: CTCATCGTGGTGGGTAACGTG R: ACACACAGCACATCTACCGAA
Beta-adrenergic receptor 2 (β2-AR)	62°C	F: GGGAACGACAGCGACTTCTT R: GCCAGGACGATAACCGACAT

Beta-adrenergic receptor 3 (β3-AR)	62°C	F: AGAAACGGCTCTCTGGCTTTG R: TGGTTATGGTCTGTAGTCTCGG
PI3K	58°C	F: CTCTCCTGTGCTGGCTACTGT R: GCTCTCGGTTGATTCCAAACT
AKT	58°C	F: CTTCCGTCCACTCTTCTCTTTC R: ATCCCCTCAACAACTTCTCAGT
MAPK	58°C	F: GGTTGTTCCCAAATGCTGACT R: CAACTTCAATCCTCTTGTGAGGG
MAPK14	58°C	F: TGACCCTTATGACCAGTCCTTT R: GTCAGGCTCTTCCACTCATCTAT
ERK1	63°C	F: TCCGCCATGAGAATGTTATAGGC R: GGTGGTGTTGATAAGCAGATTGG
ERK2	63°C	F: GGTTGTTCCCAAATGCTGACT R: CAACTTCAATCCTCTTGTGAGGG
DNMT1	60°C	F: AGAGACCAGGATAAGAAACGCA R: CTCCTTTGATTTCCGCCTCAAT
DNMT3A	60°C	F: GGCCGAATTGTGTCTTGGTG R:

		CCATCTCCGAACCACATGAC
DNMT3B	60°C	F: AGCGGGTATGAGGAGTGCAT R: GGGAGCATCCTTCGTGTCTG
MBD2	58°C	F: AGAACAAGGGTAAACCAGACCT R: ACTTCACCTTATTGCTCGGGT
GAPDH	Housekeeping Gene	F: AGGTCGGTGTGAACGGATTTG R: TGTAGACCATGTAGTTGAGGTCA

3.7. DNA isolation

During RNA isolation, chloroform was introduced and centrifuged to divide the sample into three separate phases: an aqueous phase, interphase, and phenol-chloroform phase. The aqueous contains RNA while the interphase, and phenol-chloroform phase contains DNA and proteins. DNA was extracted from the interphase and phenol-chloroform phase by precipitating with 100% ethanol (150 µl, RT, 3 min) and centrifuged (2000 xg, 4°C, 5 min). The supernatant was collected and stored for protein isolation.

To the pellets, 0.1 M sodium citrate in 10% ethanol (pH 8.5, 500 µl) was added and incubated (RT, 30 min) before centrifugation (2000 xg, 4°C, 5 min). The supernatant was removed. These steps were repeated twice. A 1000 µl of 75% ethanol resuspended the pellets before incubation (RT, 20 min) and centrifugation (2000 xg, 4°C, 5 minutes). The supernatant was removed. The pellets were air-dried (RT, 10 min). Subsequently, 100 µl of 8 mM sodium hydroxide (NaOH) buffer was added to the pellets. All insoluble materials were then removed by centrifugation (12000 xg, 4°C, 10 min).

3.7.1. DNA quantification

The ThermoFisher Scientific Nano-drop 2000 spectrophotometer was used to measure the DNA concentration and samples were standardised to 20 ng. The DNA purity was assessed by the A260/A280 absorbance ratio. At a ratio of 1.8, DNA was considered pure.

3.8. Enzyme-linked immunosorbent assay (ELISA) - Global DNA Methylation

3.8.1. Introduction

ELISA recognises and measures antibodies that passively bind to solid surfaces (Lin, 2015). The conventional ELISA involves an antigen binding to a solid surface and introducing biological material including antigen-specific antibodies covalently coupled to an enzyme (Boguszewska et al., 2019). The DNA methylation ELISA is designed to identify methylated cytosine and assess the levels of methylation using antibodies produced against 5-mC (Kurdyukov and Bullock, 2016).

A binding solution binds DNA to strip wells, therefore a high DNA affinity is achieved. Both a capture and detection antibody covalently coupled to an enzyme are needed to identify methylated DNA (Mazibuko et al., 2024). A colour shift results as the inclusion of a substrate activates enzymes (Figure 3.2). A microplate spectrophotometer measures DNA methylation through colorimetric analysis using absorbance measurements where the level of methylated DNA correlates to the optical density (Awad et al., 2020).

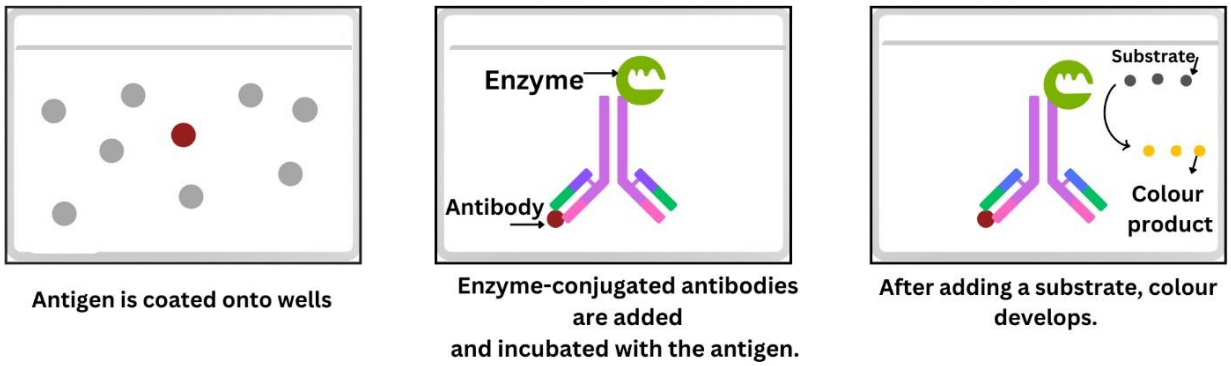

Figure 3.2: The principle of ELISA (Prepared by author using canva.com)

3.8.2. Protocol

The Methylated DNA Quantification Kit (Abcam, ab117128) measures methylated DNA. This assay quantified global DNA methylation levels (5-mC levels).

The 1x wash buffer was prepared by adding 13 ml of 10x wash buffer to 117 ml of distilled water (dH_2O).

Single-point control preparation

The positive control was diluted with 1x Tris-EDTA (TE) buffer to 5 ng/µl (1 ul of positive control and 3 µl of TE). This control was further diluted to 10 ng/µl (5 ul of positive control and 5 µl of 1x TE).

The positive control standards (0.5, 1, 2, 5, and 10 ng/µl) were prepared utilising the 10 ng/µl diluted positive control and the 1X TE Buffer (Appendix B). Before incubation (37°C, 90 min), binding solution (80 µl), positive control standards (1 µl), negative control (obtained from the kit, 1 µl), and DNA samples (8 µl) were added to strip wells in triplicate. Subsequently, the binding solution was then aspirated. Following all incubation periods, the strip wells were washed thrice with 1X Wash Buffer (150 µl). The control and PAT groups were then introduced to capture antibody (1: 1,000 (50 µl), RT, 60 min), detection antibody (1: 2,000 (50 µl), RT, 30 min), and enhancer solution (1: 5,000 (50 µl), RT, 30 min). All wells were incubated with developer solution (100 µl, RT, in the dark, 10 min) and stop solution (50 µl). Adequate amounts of 5-mC cause the developer solution to turn blue. The stop solution initiates a blue-to-yellow colour change.

3.8.3. Global DNA methylation quantification

Using the SpectroStar nano spectrophotometer (BMG Labtech) the absorbance was measured at 450 nm. The percentage of 5-mC in total DNA was calculated and expressed as a percentage compared to the control.

$$5mC\ (ng) = \frac{(Sample\ OD - Negative\ control\ OD)}{(Gradient\ of\ the\ slope\ x\ 2)}$$

$$5mC\ (\%) = \frac{5mC\ amount\ (ng)}{S}\ x\ 100\ \%$$

- Where S = input DNA (µl)

3.9. Protein isolation

3.9.1. Introduction

Employing a non-ionic lysis Cytobuster Protein Extraction Reagent, the total protein was extracted from the samples. Cytobuster contains a variety of detergents including protease and phosphatase inhibitors that facilitate the successful isolation of soluble and functional proteins. Protease and phosphatase inhibitors preserve protein integrity by inhibiting the cell from secreting proteolytic and phosphatase enzymes (Mahmood and Yang, 2012).

3.9.2. Protocol

Mice livers were homogenised with Cytobuster™ Protein Extraction Reagent (500 µl) containing protease and phosphatase inhibitors. The samples were centrifuged (4°C, 10 000 xg, 10 min). The supernatant containing the crude protein was separated from the pellet and quantified.

3.10. Bicinchoninic acid assay - Protein quantification and standardisation

3.10.1. Introduction

The Biuret reaction is the basis for the bicinchoninic acid (BCA) assay (Cortés-Ríos et al., 2020). The BCA assay operates in an alkaline medium where Cu^{2+} is converted to Cu^{+1}. This colorimetric assay measures protein quantities in samples by producing a purple Cu^{+1}-$(BCA)_2$ complex at 562 nm (Cortés-Ríos et al., 2020). The resultant Cu^{+} indicates protein concentration and thus, protein content in samples is measured spectrophotometrically by comparing it to standards with a known concentration (Cortés-Ríos et al., 2020) (Table 3.5).

3.10.2. Protocol

The 1 mg/ml bovine serum albumin (BSA) stock was prepared (5mg BSA in 5ml dH_2O). Various standards ranging from 0 to 1 mg/ml were made.

Table 3.5: BSA standards preparation

Concentration	Standards
0 mg/ml	100 µl dH_2O; 0 µl 5mg/ml BSA stock
0.2 mg/ml	80 µl dH_2O; 20 µl 5mg/ml BSA stock
0.4 mg/ml	60 µl dH_2O; 40 µl 5mg/ml BSA stock
0.6 mg/ml	40 µl dH_2O; 60 µl 5mg/ml BSA stock
0.8 mg/ml	20 µl dH_2O; 80 µl 5mg/ml BSA stock
1 mg/ml	0 µl dH_2O; 100 µl 5mg/ml BSA stock

A working solution consisting of 0.8 µl $CuSO_4$ and 39.6 µl BCA per well was prepared. In a 96- well plate, 40 µl of the working solution, in addition to 5 µl of standards, and samples were pipetted. The plate was incubated (37°C, 30 min) and read at an absorbance of 562 nm with the spectrophotometer (SpectroStar nano).

All protein samples were standardised to 1.2mg/ml and 200 µl (Appendix C). The samples were boiled (100°C, 5 min) in Laemmli buffer which consists of dH_2O which facilitated dissolution and homogenisation, 0.5 M Tris-HCl (pH 6.8) to maintain the pH level, 10% sodium dodecyl sulphate (SDS) which denatured proteins. The addition of SDS generated an overall negative charge, glycerol as it enabled the protein sample to settle to the bottom of the well by providing density to the buffer, 5% β-mercaptoethanol (2-mercaptoethanol) which facilitated protein denaturation by disrupting disulphide bridges and 1% bromophenol blue dye that determined protein migration on the gel (Sule et al., 2023).

3.11. The western blotting assay

3.11.1. Introduction

In complicated mixtures of cells or tissues, western blotting identifies and measures specific proteins to evaluate protein levels. Sodium dodecyl sulfate-polyacrylamide gel electrophoresis (SDS-PAGE) separates protein samples by molecular weight (Sule et al., 2023) (Figure 3.3). The introduction of a voltage causes negatively charged proteins on the gel to move towards the positive electrode. Smaller proteins move faster than larger ones, hence proteins are segregated by molecular weight (Mahmood and Yang, 2012) (Table 3.7). Proteins are transferred from the polyacrylamide gel onto a nitrocellulose membrane (Table 3.8). To avoid non-specific antibody binding to the membrane, it is incubated in a blocking buffer: 5% BSA in Tris buffer saline with Tween 20 (TTBS) (Mazibuko et al., 2024). By identifying antigen/antibody binding signals in biological samples, including cells and tissues, semi-quantitative or quantitative information on the protein of interest is provided (Sule et al., 2023). Bands indicate protein expression when a specific primary and enzyme-conjugated secondary antibody binds to the target protein on the membranes (Mazibuko et al., 2024).

The western blotting assay was used to determine the protein expression of p38, ERK1/2, PI3K, DNMT1, DNMT3A and MBD2.

3.11.2. Protocol

To commence the assay, the resolving and stacking gels were prepared as follows (Table 3.6):

Table 3.6: Western blot gel recipe for 4 resolving and stacking gels

Reagent	Resolving gel (10%)	Stacking gel (4%)
dH_2O	15 800 µl	12 000 µl
Tris	10 000 µl (1.5 M, pH 8.8)	5000 µl (0.5 M, pH 6.8)
10% SDS	400 µl	200 µl
Bis/Acrylamide	13 400 µl	2660 µl
10% Ammonium persulfate (APS)	200 µl	100 µl
Tetramethylethylenediamine (TEMED)	20 µl	20 µl

The proteins (30 µl) were separated using SDS-PAGE (150 V, 90 min).

Table 3.7: SDS-PAGE running buffer recipe

Reagent	Quantity
Tris	3.03 g
Glycine	14.4 g
SDS	10 g
Dissolve in dH_2O	800 ml (top up to 1000 ml)

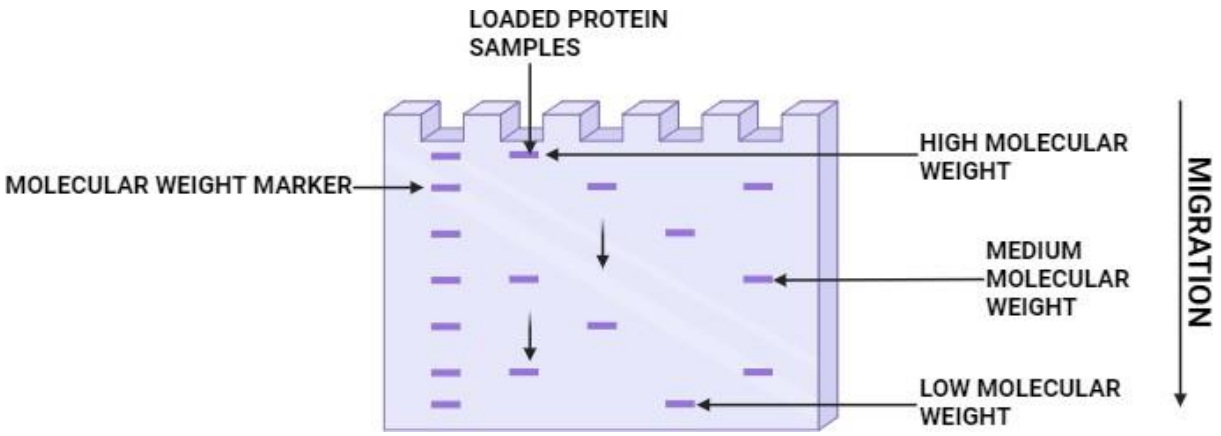

Figure 3.3: The principle of the SDS-PAGE (prepared by author using biorender.com)

Thereafter the Bio-Rad Trans-Blot® Turbo Transfer System (25 V, 30 minutes) transferred the proteins onto nitrocellulose membranes.

Table 3.8: Transfer Buffer recipe

Reagent	Quantity
Tris	1.515 g
Glycine	7.2 g
Methanol	100 ml
Dissolve in dH_2O	300 ml (top up to 500 ml)

All membranes were incubated and blocked (RT, 1 hr) using 5% BSA in 100 ml TTBS (150 mM NaCl, 3 mM KCl, 25 mM Tris, 0.05% Tween 20, distilled water, pH 7.5). Primary antibodies (1:5000 µl) such as p38 (Cell signaling Technology, #9212) and ERK1/2 (Santa Cruz Biotechnology, #sc-93; 1:5000), PI3 Kinase p110 Alpha (Proteintech, #67071-1-Ig, 1:5000), AKT (Cell Signaling Technology, 9272S, 1:5000), DNMT1 (D63A6) (Cell signaling Technology, #5032S, 1:5000), DNMT 3A (D23G1) (Cell signaling Technology, #3598S, 1:5000), and MBD2 (Abcam, ab188474, 1:5000) were added to the membrane after blocking and incubated overnight

(4°C). Following incubation, the membranes were washed five times in TTBS (RT, 10 min) (Table 3.9), introduced to a secondary antibody conjugated to horseradish peroxidase (HRP) and incubated (1 h, RT) anti-rabbit (Cell Signalling Technology, #7074S, 1:5000) and anti-mouse (Cell signaling Technology, #7076P2, 1:5000).

Table 3.9: Wash buffer- TTBS recipe

Reagent	Quantity
NaCl	8, 005 g
KCl	0.202 g
Tris	3.001 g
Dissolve in dH_2O	800 ml (top up to 1000 ml)
Tween 20	500 µl

Post-incubation the membranes underwent four TTBS washes (10 min, RT) and their protein bands were viewed with the Clarity™ Western ECL Substrate Kit (Bio-Rad, #170-5060). The images were taken with the iBright™ Imaging System (ThermoFisher, Waltham, MA, USA) (Figure 3.4). Utilising 32% hydrogen peroxide (H_2O_2) the membranes were stripped (37°C, 30 min), then washed once with TTBS (RT, 10 min), blocked with 5% BSA in TTBS and incubated (RT, 1 hr) with β-actin (Sigma-Aldrich, A3854, 1:5000) which serves as the housekeeping protein for normalisation against relevant proteins expressed. The protein bands were analysed using the iBright™ analysis software version 4.0.0 and the results were represented as relative band density (RBD) in comparison to the control.

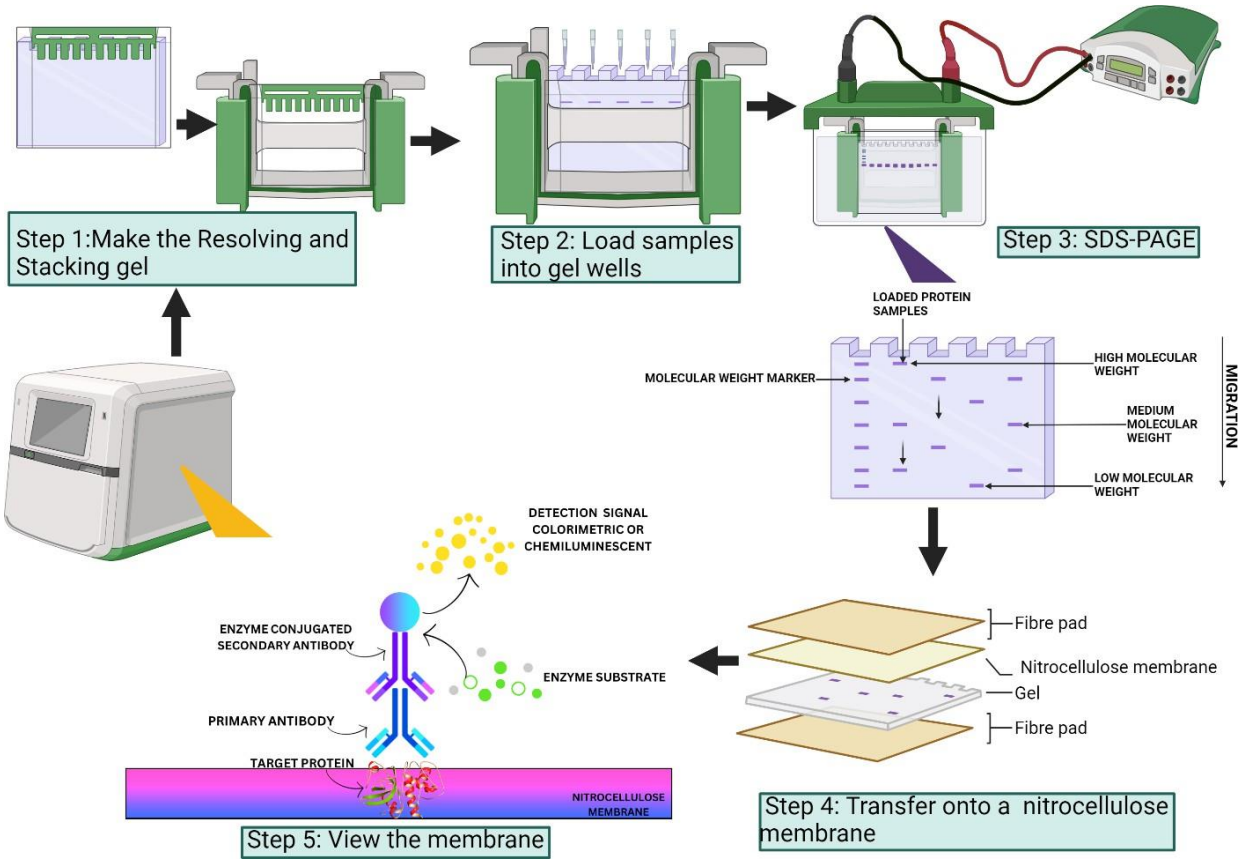

Figure 3.4: A schematic representation of the western blotting assay (prepared by author using biorender.com and canva.com)

Chapter 4: Results

4.1 PAT-modified α-adrenergic receptors mRNA levels

The mRNA levels of *α-AR*

The qPCR assay evaluated the mRNA levels of α-ARs in the livers of C57BL/6 mice that were fed PAT for 10 days. PAT altered the mRNA levels of the α-ARs by significantly increasing *α1A- AR* (p = 0,0012) (Figure 4.1a) and decreasing *α2A-AR* (p = 0,2293) (Figure 4.1b) and *α2B-AR* (p = 0,4697) (Figure 4.1c).

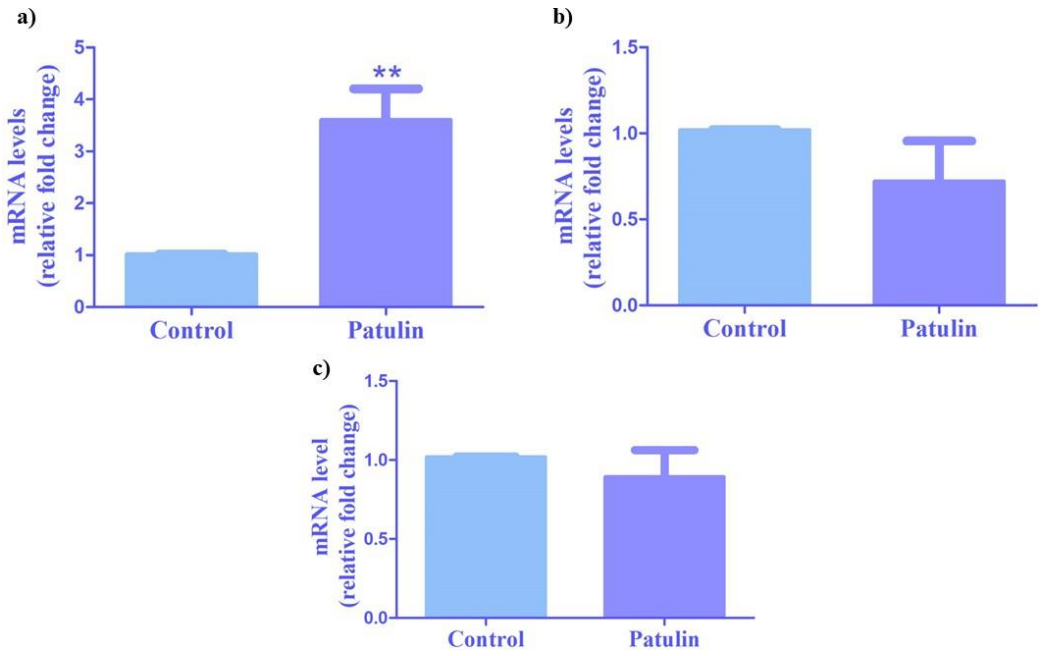

Figure 4.1: The mRNA levels of a) *α1A-AR*, b) *α2A-AR*, and c) *α2B-AR* in the livers of the control and PAT-fed C57BL/6 mice for 10 days. All data is presented as mean with SEM where (**p<0.005) was deemed significant.

4.2 PAT modified β-adrenergic receptors mRNA levels

The mRNA levels of *β-AR*

PAT had decreased the mRNA levels of all β-AR. PAT reduced the levels of *β1-AR* (p = 0,5942) (Figure 4.2a) whilst significantly decreasing the levels of *β2-AR* (p = 0,0008) (Figure 4.2b) and declining *β3-AR* (p = 0,4039) (Figure 4.2c).

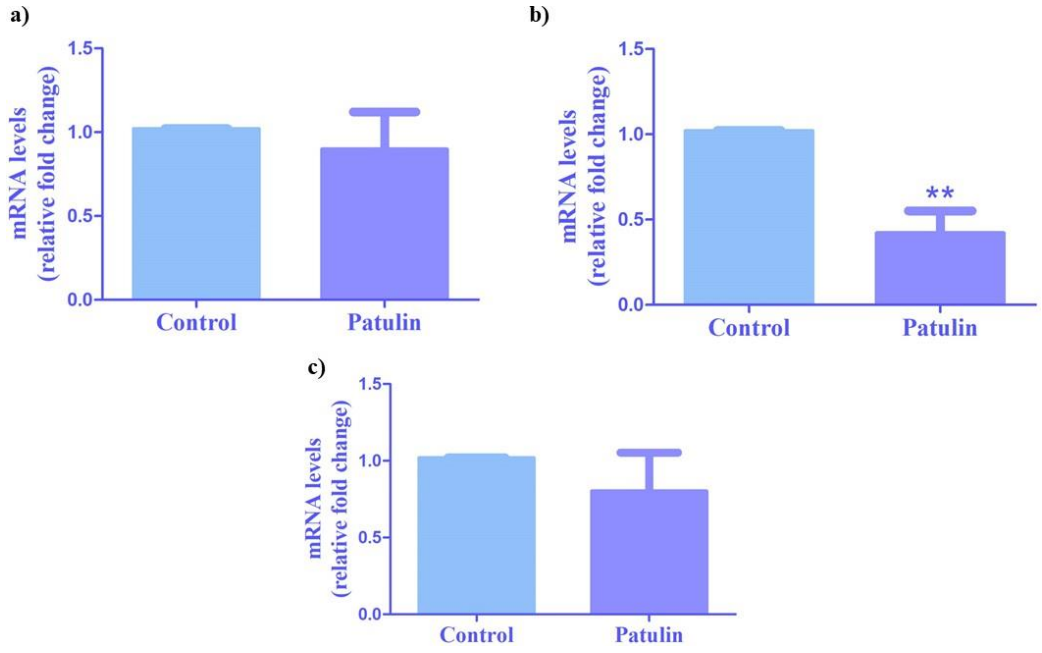

Figure 4.2: The mRNA levels of a) *β1-AR*, b) *β2-AR*, and c) *β3-AR* in the livers of the control and PAT-fed C57BL/6 mice for 10 days. All data is presented as mean with SEM where (**p<0.005) was deemed significant.

4.3. PAT disrupts the MAPK/ERK signalling pathways

PAT has dysregulated the MAPK/ERK signalling cascade by significantly increasing the mRNA levels of *MAPK* (p = 0,0262) (Figure 4.3a), *MAPK 14* (p<0.0001) (Figure 4.3b) and *ERK1* (p = 0, 0198) (Figure 4.3c). PAT significantly decreased the mRNA levels of *ERK2* (p<0.0001) (Figure 4.3d).

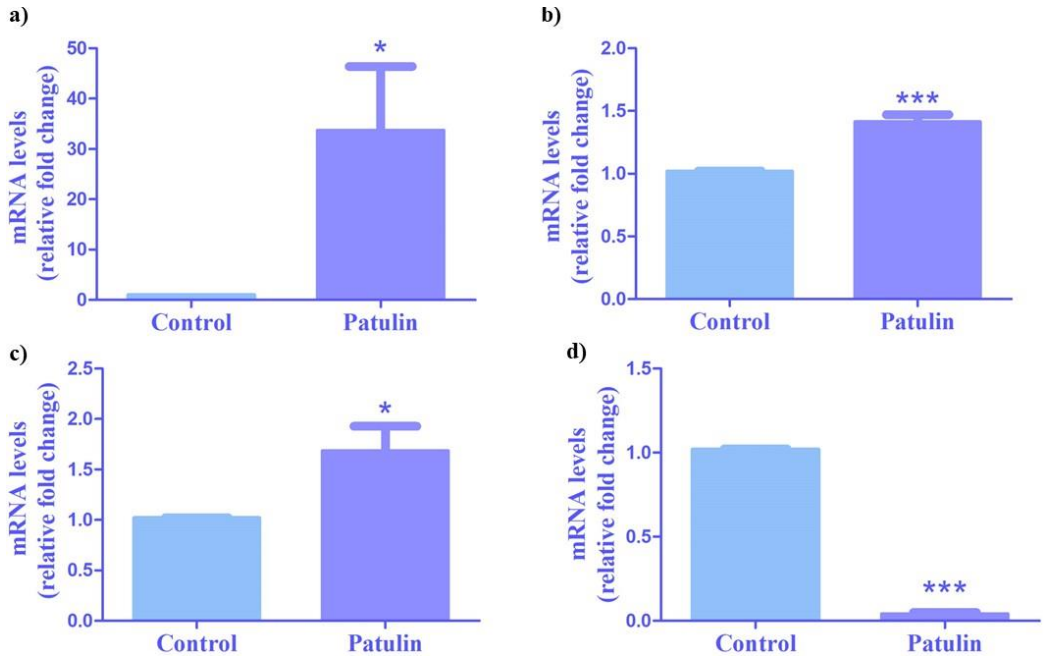

Figure 4.3: The mRNA levels of a) *MAPK*, b) *MAPK14*, c) *ERK1* and d) *ERK2* in the livers of the control and PAT-fed C57BL/6 mice for 10 days. All data is presented as mean with SEM where (*p<0.05, ***p<0.0001) was deemed significant.

4.4. PAT alters the protein expression of p38 and ERK1/2

The western blot assay demonstrated a PAT-mediated dysregulation of this pathway. This was exhibited when PAT significantly increased and decreased the protein levels of p38 (p = 0,0473) (Figure 4.4a) and ERK1/2 (p = 0,0045) (Figure 4.4b) respectively.

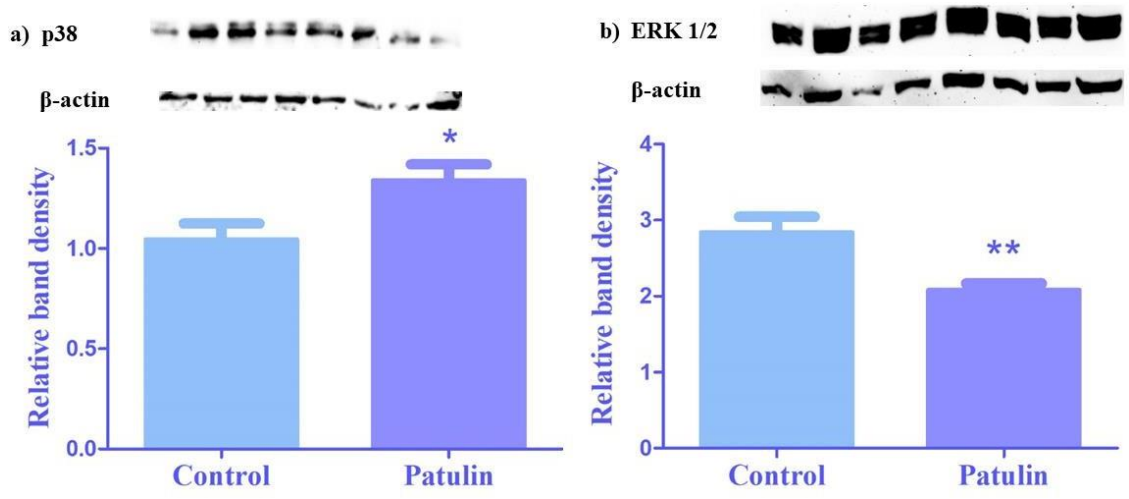

Figure 4.4: The protein levels of p38 and ERK1/2 in the livers of the control and PAT-fed C57BL/6 mouse for 10 days. All data is presented as mean with SEM where (*p<0.05, **p<0.005) was deemed significant.

4.5. PAT dysregulates PI3K/AKT signalling

PAT altered the mRNA levels of this pathway by decreasing *PI3K* (p = 0,4776) (Figure 4.5a) and significantly increasing *AKT* (p = 0,0139) (Figure 4.5b).

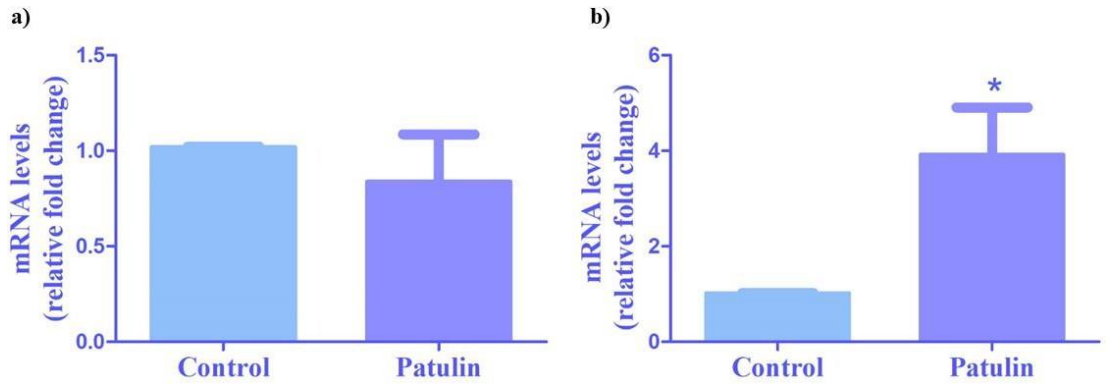

Figure 4.5: The mRNA levels of a) *PI3K* and b) *AKT* in the livers of the control and PAT-fed C57BL/6 mice for 10 days. All data is presented as mean with SEM where (*p<0.05) was deemed significant.

4.6. PAT increases PI3K protein levels

Due to the decline in mRNA levels of PI3K, the protein levels of PI3K were investigated. PAT significantly increased the protein levels of PI3K (p = 0,0373) (Figure 4.6).

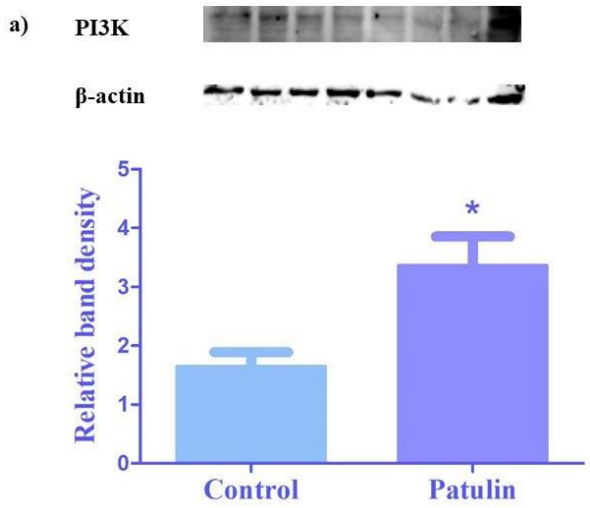

Figure 4.6: The protein levels of PI3K in the livers of the control and PAT-fed C57BL/6 mice for 10 days. All data is presented as mean with SEM where (*p<0.05) was deemed significant.

4.7. PAT induces global DNA hypermethylation

An ELISA assay was performed to measure global DNA methylation levels. PAT had significantly increased the global DNA methylation levels (p = 0,0416) (Figure 4.7).

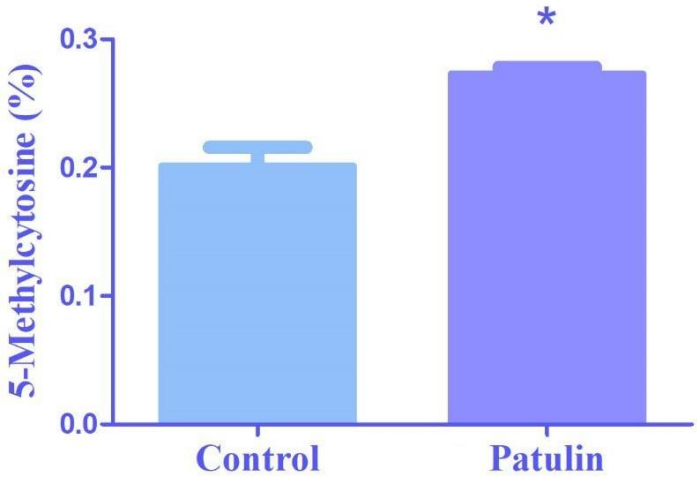

Figure 4.7: Global DNA hypermethylation as represented by the percentage (%) of 5-mC in the livers of the control and PAT-fed C57BL/6 mouse livers for 10 days. All data is presented as mean with SEM where (*p<0.05) was deemed significant.

4.8. PAT alters global DNA methylation in mouse livers

Due to the resultant global DNA hypermethylation, the levels of the DNMTs were investigated. PAT dysregulated the mRNA levels of the DNMTs by increasing *DNMT1* (p = 0,3076) (Figure 4.8a) and significantly decreasing *DNMT3A* (p< 0.0001) (Figure 4.8b) and *DNMT3B* (p< 0.0001) (Figure 4.8c).

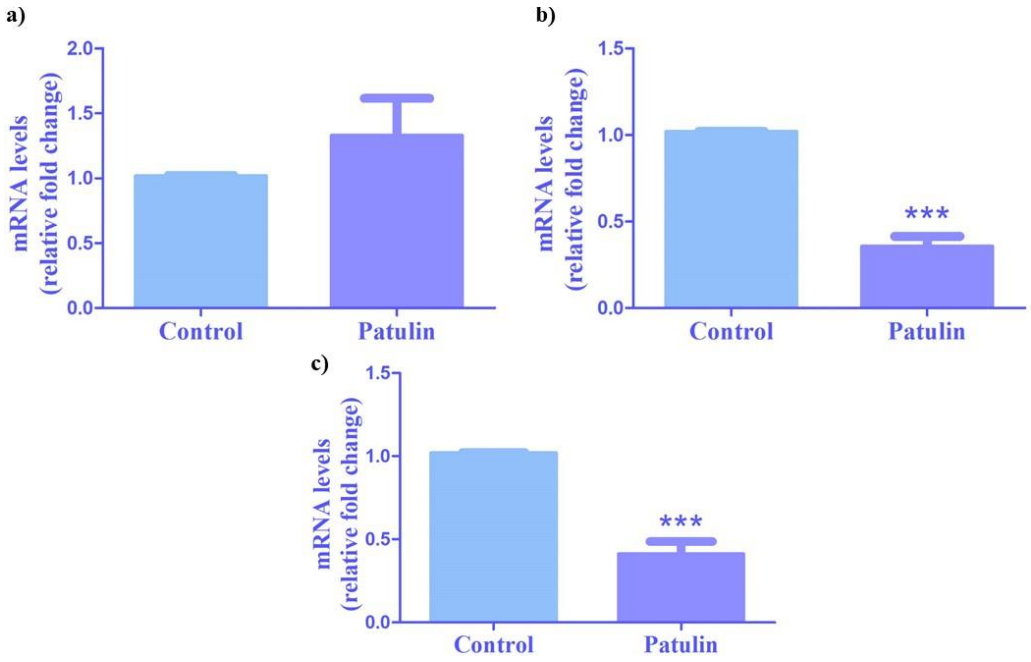

Figure 4.8: The mRNA levels of a) *DNMT1*, b) *DNMT3A* and *DNMT3B* in the livers of the control and PAT-fed C57BL/6 mice for 10 days. All data is presented as mean with SEM where (***p<0.0001) was deemed significant.

4.9. PAT increases DNMT protein levels

The dysregulated mRNA levels of the DNMTs led to the further investigation of its protein levels. PAT significantly increased the protein levels of DNMT1 (p = 0,0402) (Figure 4.9a) and DNMT3A (p = 0,6701) (Figure 4.9b).

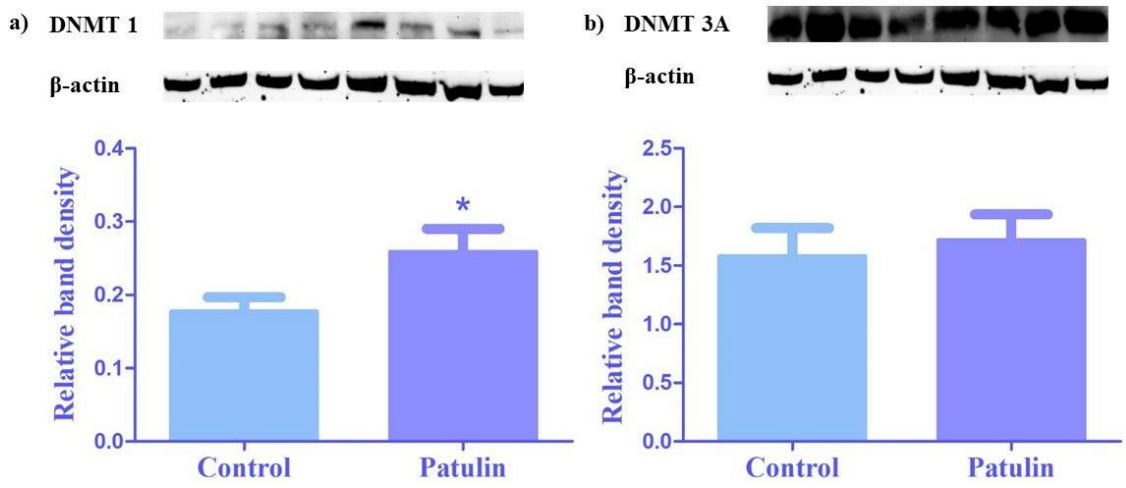

Figure 4.9: The protein levels of DNMT1 and DNMT3A in the livers of the control and PAT-fed C57BL/6 mice for 10 days. All data is presented as mean with SEM where (*p<0.05) was deemed significant.

4.10. PAT increases MBD2 levels

To determine the level of demethylation, MBD2 mRNA and protein levels were investigated. PAT increased MBD2 mRNA (p = 0, 1942) (Figure 4.10a) and protein expression levels (p = 0,0501) (Figure 4.10b).

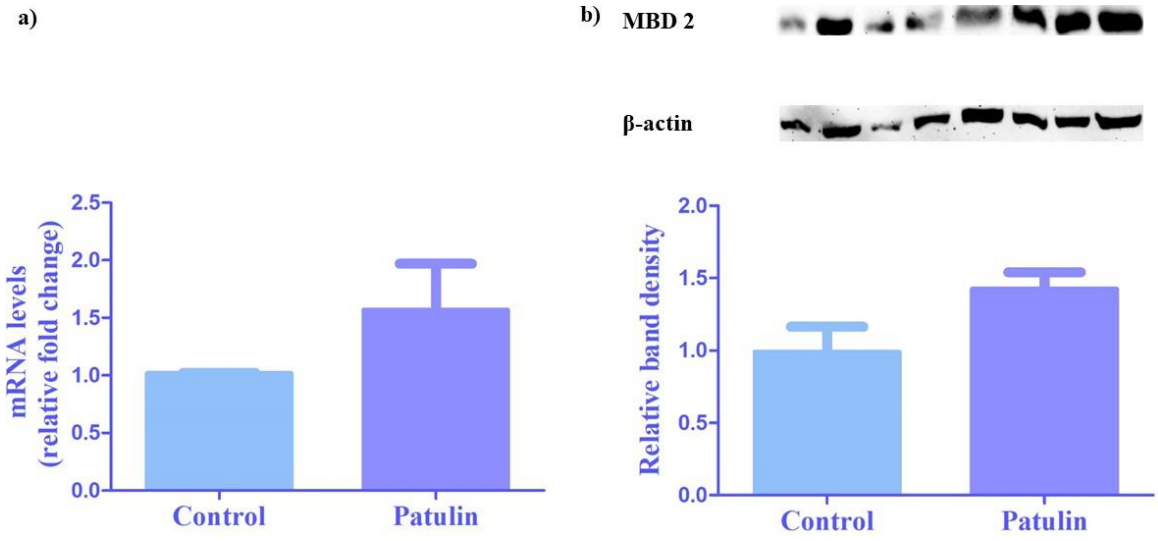

Figure 4.10: The mRNA and protein levels of MBD2 a) mRNA and b) protein in the livers of the control and PAT-fed C57BL/6 mice for 10 days.

Chapter 5: Discussion

PAT is derived from several fungi and can infect numerous food products (Guerra-Moreno and Hanna, 2017). PAT has teratogenic, carcinogenic, and genotoxic properties (Qiu et al., 2022). Additionally, PAT exposure induces acute symptoms such as liver and renal toxicity (Chu et al., 2021). This study investigated the effect of PAT on adrenergic receptor signalling and global DNA methylation. The limitations of this study include a small sample size and a lack of western blot data showing the protein expression of α and β-AR, AKT and DNMT3B.

The liver possesses α1-AR and β2-AR (Chen et al., 2020). In the liver, α1-ARs regulate liver function by mediating the action of epinephrine and norepinephrine. In liver physiology, the ARs signalling modulates a variety of processes, notably liver regeneration, repair, fibrosis and innate immunity, hepatocyte proliferation, glycogenolysis and gluconeogenesis (Chen et al., 2020). The expression of the various subtypes is governed by multiple transcriptional and post-synthetic processes at the gene, mRNA, and protein levels (Strosberg, 1993).

In C57BL/6 mouse livers, prolonged exposure (10 days) to PAT significantly increased the mRNA levels of *α1-AR* (Figure 4.1a). Following liver injury, the α1-AR regulates hepatocyte growth and liver regeneration (Aldaba-Muruato et al., 2017). As PAT primarily targets the liver and exerts its toxicity, the increase in α1A-AR levels may serve as a response to PAT-induced injury. The increased α1A-AR responds by initiating regenerative actions through hepatocyte proliferation, possibly attempting to repair any degree of harm induced by this deleterious mycotoxin. In Kupffer cells, by activating the α1-ARs the inflammatory cytokine generation was significantly increased (Huan et al., 2017). It is plausible that the α1A-AR upregulation is an inflammatory response to PAT. This provides a possible mechanism of PAT-mediated liver injury. By maintaining α1A-AR activation, the liver is in a chronic state of inflammation. Liver fibrosis alters the adrenergic receptors (Schwinghammer et al., 2020).

A protein sequence similarity of 44% was predominantly observed in the α1- and 2- AR membrane-spanning regions, in addition to other members of this receptor family (Insel, 1989). Thus, as these receptors are similar in nature, PAT binds and influences their levels possibly using a similar mechanism. The α2A and α2B-AR were not significant. This study observed a PAT-mediated decrease in the levels of *α2A-AR* (Figure 4.1b) and *α2B-AR* (Figure 4.1c). This strengthens the premise that PAT disrupts AR signalling. While most studies focused on β-AR, Link et al. observed

a similarity between human and murine α2A-ARs; that replacing Cys^{201} with Ser transmembrane (TM) region 5 resulted in the same antagonistic binding capabilities (Link et al., 1992). Interestingly PAT has mutagenic properties (Kumar et al., 2018a). This could account for the decline in α2A-AR levels, PAT may have mutated these residues in the TM region thus altering the structure of the AR and preventing its natural ligand from binding to the ARs. PAT can act as a ligand (Pillay et al., 2020). By competing for binding sites, PAT acts as a ligand and binds to the ARs thus altering their structure and hindering its ability to transduce signaling. The AR subtypes can have different effects based on tissue location, even within the same class (Wu et al., 2021). The three α2-AR isoforms share comparable structures, pharmacology, and signalling processes, but differ in tissue distribution, despite having only about 50% amino acid sequence commonality (Pettinger and Jackson, 2020). Renal α-AR regulates metabolism, sodium reabsorption, and renal tone (Mazibuko et al., 2024).

Recent studies have observed similar trends in AR signalling following PAT exposure in two different kidney models. A study by Mazibuko et al. investigated the effect of PAT on adrenergic receptor signalling and DNA methylation in C57BL/6 mouse kidneys for two timeframes acute (1 day) and chronic (10 days). At 2.5 mg/kg, in both acute and chronic exposures, PAT resulted in a significant decline of *α1A-AR*, *α2A-AR*, and *α2B-AR* levels (Mazibuko et al., 2024). Pillay et al. investigated PAT's effect (2.5 μM) on the α-AR signalling in HEK 293 cells for 24 hrs (Pillay et al., 2020). PAT significantly reduced the mRNA levels of *α1A*, *α2A* and *α2B*-ARs in HEK293 cells (Pillay et al., 2020).

Mazibuko et al. suggested that the increase in α2-AR is the kidney's response to the presence of PAT. Additionally, the activation of the α2-AR influences blood pressure through renal vasoconstriction thus affecting overall kidney function (Mazibuko et al., 2024). In HEK293 cells PAT had significantly decreased the protein level of α1A-AR (Pillay et al., 2020).

Additionally, Pillay et al. employed computational methods to investigate the interaction between PAT and human α1A-AR (Pillay et al., 2020). The study's findings indicated that by using hydrogen, pi-pi, and pi-alky bonding, PAT binds and interacts with α1-AR residues. PAT interacts with the side chains of non-thiol amino acids, including Ser, tyrosine (Tyr), phenylalanine (Phe), glutamic acid (Glu), and lysine (Lys) thus binding to α1-AR (Pillay et al.,

2020). Aspartic acid^{113} (Asp) is the most significant residue found in all adrenergic receptors (Dixon et al., 1988). Asp does not possess a thiol group (Anon., 2022). All adrenergic receptors possess key residues for ligand binding, namely Asp^{113}, Ser^{204}, and Ser^{207} which are found in the same locations (Dixon et al., 1988, Isin et al., 2013, Catte et al., 2022). Whilst there is no literature on this subject, this study postulates that the decline in the livers'α- and β-AR levels is attributed to PAT mutating the Asp residue, thus affecting the receptors' affinity and efficiency in ligand binding. Another possible explanation includes PAT binding to the Asp residue in the ARs, thus altering their expression level and disrupting their signalling.

The disruption in adrenergic signalling trends is possibly due to epigenetic modifications, specifically altered DNA methylation levels which impact gene transcription and thus receptor levels. Liver injury can alter regular cellular activities and signalling pathways, hence the possibility of affecting the activity of the ARs in the liver.

In the case of the β-ARs, PAT decreased the mRNA levels of all three β-ARs: *β1* (Figure 4.2a), *β2* (Figure 4.2b) and *β3* (Figure 4.2c). The β1 and β3-AR were not significant however, β2-AR exhibited a significant decrease. In NAFLD- induced fibrosis, all β-ARs are reduced during the early phases, but with increasing fibrosis/cirrhosis stages, their levels are significantly increased (Schwinghammer et al., 2020). Therefore, the decline in β-ARs levels observed in this study is a possible indicator of the liver experiencing the initial stages of fibrosis following PAT exposure.

Interestingly, the presence of Cys residues in similar places within the β-AR is practically in all GPCRs, suggesting that their binding may be a common component of the R7G family of proteins (Strosberg, 1993). Therefore, the decrease in all three β-ARs may be attributed to PAT targeting Cys residues present in the ARs, as PAT has an affinity for Cys (Pal et al., 2017).

Strosberg (1993) reviews the effects of mutations on the ARs. Ligand binding is altered when residues are mutated in various TM regions particularly Ser^{165} (TM4), Phe^{290} (TM6), and the four Cys residues Cys^{106}, Cys^{184}, Cys^{190}, and Cys^{191} (Strader et al., 1987, Dixon et al., 1988). This correlates with the findings of Pillay et al. as PAT has interacted with the ARs through Ser and Phe residues (Pillay et al., 2020).

Position 113 of the receptors are critical for its function. Substituting aspartate with serine results in catechol esters interacting with the residue's hydroxyl group through a hydrogen bond

thus serving as agonists for the mutated receptor (Strader et al., 1991). Therefore, it is plausible for PAT to alter the AR structure and its function in activating downstream signalling.

GPCRs can stimulate the MAPK/ERK signalling cascades (Moon and Ro, 2021). An investigation on α1-AR-ligand binding revealed that receptor engagement can directly activate or induce parallel stimulation of MAPK/ERK1/2 (Pillay et al., 2020). The MAPK/ERK and PI3K/AKT pathways require both α1 and α2-ARs to function properly (Mazibuko et al., 2024). Studies have demonstrated that activating β-AR enables the formation and stimulation of signalling cascades, notably MAPK pathways (Vasudevan et al., 2011). Consequently, any AR dysregulation impacts the cascades as mentioned above.

The mRNA and protein levels of the MAPK/ERK/PI3K/AKT pathways utilised by the adrenergic receptors were investigated in C57BL/6 mouse livers.

A wide range of substrates are phosphorylated by MAPK/ERK signalling in the cytoplasm and nucleus, facilitating various biological functions (Wen et al., 2022). Injuries swiftly trigger MAPK/ERK signalling pathways. Subsequently, this pathway has a significant role in organ regeneration by stimulating cell survival, migration, transcription/translation, growth and proliferation (Wen et al., 2022). PAT significantly increased the mRNA levels of *MAPK* (Figure 4.3a), *MAPK14* (Figure 4.3b) and *ERK1* (Figure 4.3c). This significant upregulation is a possible response to PAT-mediated injury and an initiation of liver regeneration.

However, PAT significantly downregulated *ERK2* mRNA levels (Figure 4.3d). PAT decreased the protein ERK1/2 level significantly (Figure 4.4b). Essential biological functions including cellular differentiation proliferative actions and cellular signalling are governed by ERK1 and ERK 2 during healthy and pathological circumstances (Guo et al., 2020). Small variations in ERK 1/ERK2 expression can affect global ERK levels. Comparing ERK1 and ERK2 morpholinos revealed that ERK2 substantially decreased the global expression of phospho-ERK (Buscà et al., 2016). This explains how a PAT-mediated reduction of *ERK2* mRNA levels decrease the overall ERK1/2 protein expression. Any abnormalities in the ERK cascade exert deleterious effects on cells and the organism (Guo et al., 2020). Dysfunctional signalling cascades are linked to the onset of cancer (Bahar et al., 2023). This is a possible mechanism of how PAT induces liver injury which may result in liver cancer.

Additionally, PAT further disrupted the MAPK/ERK signalling cascade by significantly increasing the protein levels of P38 (Figure 4.4a). The kinase p38 is multifunctional, modulating various physiological activities by engaging with an array of substrates. These activities include cell growth, differentiation, stress response, apoptosis, and cell migration and survival (Martínez-Limón et al., 2020). Maintaining p38 activation can result in cell death, senescence, and the terminal differentiation of cells, while cell survival is promoted by low p38 activity (Martínez- Limón et al., 2020). Therefore, the p38 activation could be attributed to PAT-mediated apoptosis or a response to the stress induced in the liver upon PAT administration. Increased p38 MAPK activation is associated with liver cancer progression (Burton et al., 2021). Additionally, a PAT- mediated increase in p38 in the liver may be an example of PAT's carcinogenic properties.

Mazibuko et al. reported that in acute and chronic timeframes, PAT significantly increased the mRNA and protein levels of MAPK (Mazibuko et al., 2024). While the mRNA levels of *MAPK 14* exhibited a PAT-mediated increase in acute and chronic exposures (Mazibuko et al., 2024). Additionally, in these timeframes, PAT significantly elevated the protein level of ERK1/2, which they attribute to α1-AR mediated activation through endocytic mechanisms (Mazibuko et al., 2024). In addition to the effect of PAT on ARs, Pillay et al. (2020) investigated the effect of PAT (0.2, 0.5, 1 µM) on the MAPK/ERK/PI3K/AKT pathways in HEK293 cells. Their study reported that 1 µM of PAT significantly reduced and raised total ERK1/2 and pERK1/2 protein levels, respectively. This was associated with changes in α1-AR expression (Pillay et al., 2020).

Various mechanisms can cause liver injury, but abnormal signalling is a key factor (Vinken et al., 2009). Regulatory variables, including growth factors, cytokines, epigenetic alterations, ligand-receptor relationships, oncogenes and subcellular compartment localisations, affect MAPK/ERK signalling activity (Guo et al., 2020, Wen et al., 2022). As exhibited by Pillay et al. PAT acts as a ligand and binds to the ARs, thus the adrenergic receptor levels and their signalling cascades are disrupted (Pillay et al., 2020). Insufficient or dysregulated signalling activity in mammalian cells contributes to impaired regeneration capabilities (Wen et al., 2022). Therefore, as PAT disrupts these signalling cascades, liver regeneration is possibly impaired and may ultimately lead to liver failure. Additionally, aberrant cell actions occur when the MAPK/ERK pathway is abnormally regulated, comprising accelerated cellular proliferation, longevity and reverse differentiation, thereby promoting cancer (Moon and Ro, 2021).

Studies have reported that the PI3K/AKT pathway is predominantly stimulated by MAPK/ERK crosstalk (Pillay et al., 2020). Therefore, any abnormalities in the MAPK/ERK pathway disrupt this cascade's downstream targets, particularly PI3K/AKT.

The PI3K/AKT signalling pathway regulates the body's physiological processes for suitable cellular responses to several triggers (Shamsan et al., 2024). This cascade influences survival, proliferation, cell growth, and metabolism as well as promotes liver regeneration. PI3K regulates AKT. Stimulated PI3K promotes PIP_2 to PIP_3 conversion, which promotes PDK1 and AKT activation (Xue et al., 2021). AKT activation leads to reduced inflammation as well as better repair of liver fibrosis (Shamsan et al., 2024). Thus, indicating a directly proportional or dependent relationship between PI3K and AKT. The PI3K/AKT pathway regulates the progression and attenuation of liver fibrosis thus exhibiting its duality (Shamsan et al., 2024). Activating PI3K/AKT reduces fibrosis indicators and improves liver function significantly; however, dysregulation of this pathway induces and exacerbates liver fibrosis (Shamsan et al., 2024). This study reports that PAT has disrupted the PI3K/AKT pathway. The *PI3K* mRNA levels had decreased but were not significant (Figure 4.5a). PAT significantly increased *AKT* expression (Figure 4.5b). AKT and mTOR- dependent feedback reduce receptor synthesis and signalling, which limits the PI3K signal (Mukherjee et al., 2021). The increase in AKT could serve as a negative feedback loop resulting in the decline of AR and PI3K levels.

Additionally, PAT significantly increased the protein expression of PI3K (Figure 4.6). Compared to the mRNA levels, the protein levels are more preserved in species, which could account for the lack of correlation in the expression (Jiang et al., 2023). It is possible that the dysregulation of this pathway induced liver fibrosis and another mechanism was employed for PAT-mediated toxicity. AKT serves as an effector in the PI3K pathway. It favours cell viability by phosphorylating and hindering proteins that promote apoptosis including BAD and caspase-9 (Shamsan et al., 2024). Therefore, following PAT administration, liver cancer may result through AKT-mediated anti-apoptotic actions.

After translation, the genome is regulated by small non-coding RNAs called microRNAs (miR) (Segal and Slack, 2020). The miRs downregulate mRNA by binding to sites often found in the target mRNA's 3'-untranslated region (UTR) but can also exist in the 5'UTR (Lytle et al., 2007).

The PI3K/AKT/mTOR pathway can be miR-regulated (Rahmani et al., 2020a, Rahmani et al., 2020b). The miR-519a targets PI3K/AKT in hepatocellular carcinoma (Tu et al., 2016). Tu et al. demonstrated an increase in the mRNA and protein levels of phosphatase and tensin homolog (PTEN) by inhibiting miR-519a (Tu et al., 2016). The PI3K/AKT cascade is negatively influenced by the membrane-bound lipid phosphatase, PTEN (Nie et al., 2018). By inhibiting PI3K activity, PTEN hinders PIP_2 transformation to PIP_3 (Acosta-Martinez and Cabail, 2022). Hence PAT may downregulate miR-519a which indirectly influences PI3K levels by directly upregulating PTEN. To validate this inverse relationship, Wan et al. reported that *in vitro* models of non-small cell lung cancer (NSCLC), at elevated levels of miR-142-5p reduced the protein levels of PTEN while increasing PI3K, p-Akt expression (Wan et al., 2018).

Furthermore, dysregulated PI3K/AKT/mTOR signalling is crucial in carcinogenesis (Jiang et al., 2020, Liu et al., 2020). In lung adenocarcinoma, miR-200 is upregulated and promotes tumour proliferation by stimulating AKT through insulin receptor substrate-1 (Guo et al., 2015). In their study, Nie et al. reported PTEN as a direct target of miR-217 in cardiac hypertrophy (Nie et al., 2018). An upregulation of miR-217 leads to decreased PTEN and increased AKT levels (Nie et al., 2018). Therefore, a possible explanation for the elevated mRNA levels of *AKT*, despite the decline in the mRNA levels of *PI3K*, is that PAT indirectly activates AKT by upregulating miR- 200 or miR-217. Furthermore, this upregulation of miR-200 could increase the proliferation of aberrant liver cells, thus initiating tumorigenesis.

Similarly, in mouse kidneys, the acute and chronic exposures resulted in PAT significantly decreasing and increasing the mRNA levels of *PI3K* and *AKT*, respectively (Mazibuko et al., 2024). In contrast to this study and Mazibuko et al, the findings of the western blot assay, performed by Pillay et al. reported a significant reduction in PI3K (p110γ), pAKT and AKT expression (Pillay et al., 2020). PAT-reduced PI3K/AKT activation possibly inhibits kidney metabolism and proliferation as a means of energy conservation (Pillay et al., 2020).

Multiple studies have observed mycotoxins altering DNA methylation patterns (Zhu et al., 2014, Ghazi et al., 2020, Sugiyama et al., 2021, Li et al., 2023, Mazibuko et al., 2024). During an ELISA, PAT significantly increased global DNA methylation (Figure 4.7). Therefore this study investigated the levels of the DNMTs and MBD2 using the qPCR and western blotting assay.

Regarding the expression of DNMTs, PAT elevated the mRNA levels of *DNMT1* but not significantly (Figure 4.8a). In inflammatory disorders, *DNMT1* and *MBD2* mRNA levels increase (Mazibuko et al., 2024). This possibly indicates that inflammatory processes are triggered as a response to the presence of PAT in the liver.

However, PAT significantly reduced the expression of *DNMT3A* (Figure 4.8b) and *DNMT3B* (Figure 4.8c). The chromatin structure can be modified by epigenetic alterations thus altering transcription levels even when the stressor is removed (Kumar et al., 2018b). The buildup of SAH hinders DNMT activity and impedes DNA methylation mechanisms (Ghazi et al., 2020).

However, PAT increases the protein expression of DNMT1 significantly (Figure 4.9a) however the protein levels of DNMT3A did not significantly increase (Figure 4.9b). The difference in mRNA and protein levels is possibly attributed to the Western blotting assay's ability to detect particular amino acids in post- translationally modified proteins such as methylated proteins that arise from physiologically altered normal and diseased cells (Sule et al., 2023). Chromatin modification is mediated through post-translational modifications including DNA methylation; thus, genes and proteins are influenced by epigenetic changes (Bind et al., 2022, Shu et al., 2023). Research by Fabbri et al. demonstrates a negative correlation between the levels of miR-29b and DNMT 3A and -3B mRNA levels in lung cancer tissues (Fabbri et al., 2007). DNMT 3A and DNMT 3B are targeted by miR-29b (Ghazi, 2019). Some studies have reported that the upregulation of miR-29b leads to a reduction in the mRNA levels of *DNMT3A* and *DNMT3B* (Fabbri et al., 2007, Ghazi, 2019). Therefore, it is plausible that a PAT-mediated upregulation of miR-29b reduces *DNMT3A* and *DNMT3B* mRNA levels.

The mRNA and protein levels of MBD2 exhibited a PAT-induced increase (Figure 4.10a) although not significantly. Demethylation homeostasis is achieved by elevated levels of DNMT1, DNMT3A and DNMT3B which are responsible for activating and preserving methylation and the occurrence of the MBD proteins (Menezo et al., 2016). Given the PAT-mediated dysregulation of DNA methylation, a possible explanation for the resultant global DNA hypermethylation includes raised homoCys levels, defective DNMT3B, or the direct inhibition of the transmethylase, methionine synthase (Bönsch et al., 2006).

DNMT1 maintains global methylation post-replication (Ghazi et al., 2020). It is possible that despite the downregulation in *DNMT3A* and *DNMT3B* mRNA levels, the elevated DNMT1 mRNA and protein levels account for the global DNA hypermethylation observed.

Epigenetic alterations can result in the onset of disease (Shu et al., 2023). DNA methylation was discovered to serve a crucial function in mycotoxin-induced tumorigenesis (Li et al., 2023). Aberrant DNMTs lead to incohesive DNA methylation trends which have been linked to various illnesses as well as cancer aetiology (Ghazi, 2019). It is a valid epigenetic marker for the detection of cancer (Li et al., 2023).

DNA methylation is greatly dysregulated (Ghazi et al., 2020). Previous research has indicated that mycotoxins impair DNMT expression and activity (Zhu et al., 2014, Ghazi et al., 2020, Sugiyama et al., 2021, Mazibuko et al., 2024). Regarding the epigenetic mechanism, PAT affects DNA methylation in C57BL/6 mice kidneys during acute and chronic timeframes. PAT significantly increased the mRNA levels of *DNMT1* and decreased *DNMT3A* (Mazibuko et al., 2024). PAT significantly decreased *DNMT3B* mRNA levels in acute and chronic exposures. In mice kidneys, PAT elevated *MBD2* levels during these timeframes (Mazibuko et al., 2024). As a result, global DNA hypomethylation was observed in both exposures in C57BL/6 mice kidneys, due to the increased *DNMT1* and *MBD2* levels (Mazibuko et al., 2024).

Chapter 6: Conclusion

PAT contaminates apples and apple-based products, which threatens food safety and security. This study exhibits the detrimental effects of PAT on the liver if the concentration is raised to 2.5 µM. At 2.5 µM, PAT disrupts α and β-AR levels and their MAPK/ERK/PI3K/AKT signalling pathways in C57BL/6 mouse livers. The dysregulation of these signalling cascades has been associated with liver injury, exacerbation of liver fibrosis and carcinogenesis. PAT-induced global DNA hypermethylation in C57BL/6 mouse livers. Aberrant DNA methylation has been linked to the pathophysiology of diseases, including cancer.

Therefore, PAT exerts its toxic effects in the liver by dysregulating the adrenergic receptors, MAPK/ERK/PI3K/AKT signalling pathways, as well as DNA methylation patterns. Alterations in these pathways have an overall negative impact on human health, specifically when exposed to food and beverages with PAT levels that exceed the regulatory limits of 50 µg/kg. Future studies should undertake more research on the effects of PAT on the protein levels of α and β-AR, AKT, and DNMT 3B, using western blotting. However, further investigations are required to determine a direct link between liver injury and particular changes in adrenergic receptor function and expression, in addition to the following pathways: inflammation, fibrosis, and cancer. Furthermore, investigating the effects of PAT on AR promoter methylation would provide insight into how PAT affects adrenergic receptor expression at the epigenetic level.

References

Abia, W. A., Warth, B., Ezekiel, C. N., et al. 2017. Uncommon toxic microbial metabolite patterns in traditionally home-processed maize dish (fufu) consumed in rural Cameroon. *Food and Chemical Toxicology*, 107. Available: https://doi.org/10.1016/j.fct.2017.06.011.

Acosta-Martinez, M. & Cabail, M. Z. 2022. The PI3K/Akt Pathway in Meta-Inflammation. *International Journal of Molecular Sciences, 23*. Available: https://doi.org/10.3390/ijms232315330

Adams, G. 2020. A beginner's guide to RT-PCR, qPCR and RT-qPCR. *The Biochemist,* 42. Available: https:// doi: 10.1042/BIO20200034.

Aldaba-Muruato, L. R., Muñoz-Ortega, M. H., Macías-Pérez, J. R., et al. 2017. Adrenergic regulation during acute hepatic infection with Entamoeba histolytica in the hamster: involvement of oxidative stress, Nrf2 and NF-KappaB. *Parasite*, 24.Available: https://doi.org/10.1051/parasite/2017048.

Anon. 2022. Available: https://bio.libretexts.org/@go/page/25297 [Accessed: 17 November 2024].

Antônio José, R., Rafael De Souza, M., Antônio Juscelino Sudário, S., et al. 2016. Guidelines for Successful Quantitative Gene Expression in Real- Time qPCR Assays. In: Ali, S. (ed.) *Polymerase Chain Reaction for Biomedical Applications*. Rijeka: Intech Open. Available: DOI: 10.5772/65850

Awad, A. M., Ragab, W. S., Degheidy, N., et al. 2020. Whole Genome 5'-Methylcytosine Level Quantification in Cirrhotic HCV-Infected Egyptian Patients with and without Hepatocellular Carcinoma. *International Journal of Genomics*, 2020.DOI: 10.1155/2020/1769735

Awuchi, C., Nwozo, S., Salihu, M., et al. 2022a. Mycotoxins' toxicities-from consumer health safety concerns, to mitigation/treatment strategies: A perspective review. *Journal of Chemical Health Risks*, 4. DOI: 10.22034/jchr.2022.1939170.1399

Awuchi, C. G., Ondari, E. N., Nwozo, S., et al. 2022b. Mycotoxins Toxicological Mechanisms Involving Humans, Livestock and Their Associated Health Concerns: A Review. *Toxins (Basel)*, 24. DOI: 10.3390/toxins14030167

Awuchi, C. G., Owuamanam, C. I., Ogueke, C. C., et al. 2019. Evaluation of Patulin Levels and impacts on the Physical Characteristics of Grains. *International Journal of Advanced Academic Research, Evaluation*, 5. ISSN: 2488-9849

Bahar, M. E., Kim, H. J. & Kim, D. R. 2023. Targeting the RAS/RAF/MAPK pathway for cancer therapy: from mechanism to clinical studies. *Signal Transduction and Targeted Therapy*, 8.DOI: 10.1038/s41392-023-01705-z

Bind, S., Bind, S., Sharma, A. K., et al. 2022. Epigenetic Modification: A Key Tool for Secondary Metabolite Production in Microorganisms. *Frontiers in Microbiology*, 13. Available: https://doi.org/10.3389/fmicb.2022.784109.

Birkinshaw, J. H., Bracken, A., Michael, S. E. et al. 1943. II. Biochemistry and Chemistry. *The Lancet*, 242. Available: https://doi.org/10.1016/S0140- 6736(00)88177-5

Bissessur, J., Permaul, K. & Odhav, B. 2001. Reduction of Patulin during Apple Juice Clarification. *Journal of Food Protection*, 64. Available: https://doi.org/10.4315/0362-028X-64.8.1216

Boguszewska, K., Szewczuk, M., Urbaniak, s., et al. 2019. Review: immunoassays in DNA damage and instability detection. *Cellular and Molecular Life Sciences*, 76. DOI: 10.1007/s00018-019-03239-6

Bönsch, D., Lenz, B., Fiszer, R., et al. 2006. Lowered DNA methyltransferase (DNMT-3b) mRNA expression is associated with genomic DNA hypermethylation in patients with chronic alcoholism. *Journal of Neural Transmission* (Vienna, Austria: 1996), 113. DOI: 10.1007/s00702-005-0413-2

Burton, J. C., Antoniades, W., Okalova, J., et al. 2021. Atypical p38 signaling, activation, and implications for disease. *International Journal of Molecular Sciences*, 22. DOI: 10.3390/ijms22084183

Buscà, R., Pouysségur, J. & Lenormand, P. 2016. ERK1 and ERK2 Map Kinases: Specific Roles or Functional Redundancy? *Frontiers in Cell and Developmental Biology*, 4. Available: https://doi.org/10.3389/fcell.2016.00053

Catte, A., Biswas, A. D., Mancini, G. et al. 2022. L-DOPA and Droxidopa: From Force Field Development to Molecular Docking into Human β (2)-Adrenergic Receptor. *Life (Basel)*, 12, Doi: 10.3390/life12091393.

Chain, E., Florey, H. W. & Jennings, M. A. 1942. An Antibacterial Substance Produced by Penicillium claviforme. *British Journal of Experimental Pathology*, 23. ISSN: 0007-1021

Chen, G., Fan, X., Li, Y., et al. 2020. Promoter aberrant methylation status of ADRA1A is associated with hepatocellular carcinoma. *Epigenetics*, 15. Doi: 10.1080/15592294.1709267

Chu, Q., Wang, S., Jiang, L., et al. 2021. Patulin induces pyroptosis through the autophagic-inflammasomal pathway in liver. *Food and Chemical Toxicology*, 147. https://doi.org/10.1016/j.fct.2020.111867

Cortés-Ríos, J., Zárate, A. M., Figueroa, J. D., et al. 2020. Protein quantification by bicinchoninic acid (BCA) assay follows complex kinetics and can be performed at short incubation times. *Analytical Biochemistry*, 608. Doi: 10.1016/j.ab.2020.113904

Dailey, R., Brouwer, E., Blaschka, A., et al. 1977. Intermediate-duration toxicity study of patulin in rats. *Journal of Toxicology and Environmental Health*, Part A Current Issues, 2. DOI: 10.1080/15287397709529471

Delidow, B. C., Lynch, J. P., Peluso, J. J., et al. 1993. Polymerase chain reaction: basic protocols. *Methods in Molecular Biology*, 15.https://doi.org/10.1385/0-89603-244-2:1

Dixon, R. A., Sigal, I. S. & Strader, C. D. 1988. Structure-function analysis of the beta-adrenergic receptor. *Cold Spring Harbor Symposia on Quantitative Biology*, 53. Doi: 10.1101/sqb.1988.053.01.056.

Duncan, H., Mercader, J. V., Agulló, C., et al. 2021. Chemical strategies for triggering the immune response to the mycotoxin patulin. *Scientific Reports*, 11. DOI: 10.1038/s41598-021-02916-6.

Fabbri, M., Garzon, R., Cimmino, A., et al. 2007. MicroRNA-29 family reverts aberrant methylation in lung cancer by targeting DNA methyltransferases 3A and 3B. *Proceedings of the National Academy of Sciences of the United States of America*, 104. Doi: 10.1073/pnas.0707628104.

Freitas, F. C. P., Depintor, T. S., Agostini, L. T., et al. 2019. Evaluation of reference genes for gene expression analysis by real-time quantitative PCR (qPCR) in three stingless bee species (Hymenoptera: Apidae: Meliponini). *Scientific Reports*, 9. Doi: 10.1038/s41598-019-53544-0

Frizzell, C., Elliott, C. T. & Connolly, L. 2014. Effects of the mycotoxin patulin at the level of nuclear receptor transcriptional activity and steroidogenesis in vitro. *Toxicology Letters*, 229. Doi: 10.1016/j.toxlet.2014.06.847

García-Guede, Á., Vera, O. & Ibáñez-De-Caceres, I. 2020. When Oxidative Stress Meets Epigenetics: Implications in Cancer Development. *Antioxidants* (Basel), 9. Doi: 10.3390/antiox9060468.

Ghazi, T. 2019. *Fusaric Acid-induced Epigenetic Modifications in Vitro and in Vivo: Alternative Mechanisms of Hepatotoxicity*. Ph.D. University of KwaZulu-Natal, Durban. https://books.google.co.za/books?id=mXLpzQEACAAJ

Ghazi, T., Arumugam, T., Foolchand, A. et al. 2020. The Impact of Natural Dietary Compounds and Food-Borne Mycotoxins on DNA Methylation and Cancer. *Cells*, 9. DOI: 10.3390/cells9092004

Ghosh, P. M., Shu, Z. J., Zhu, B., et al. 2012. Role of β-adrenergic receptors in regulation of hepatic fat accumulation during aging. *Journal of Endocrinology*, 213. Doi: 10.1530/JOE-11-0406

Giltrow, E., Eccles, P. D., Hutchinson, T. H., et al. 2011. Characterisation and expression of β1-, β2- and β3-adrenergic receptors in the fathead minnow (Pimephales promelas). *General and Comparative Endocrinology*, 173. Doi: 10.1016/j.ygcen.2011.07.006.

Glaser, N. & Stopper, H. 2012. Patulin: Mechanism of genotoxicity. *Food and Chemical Toxicology*, 50. Doi: 10.1016/j.fct.2012.02.096

Guerra-Moreno, A. & Hanna, J. 2017. Induction of proteotoxic stress by the mycotoxin patulin. *Toxicology Letters*, 276. Doi: 10.1016/j.toxlet.2017.05.015

Guo, L., Wang, J., Yang, P., et al. 2015. MicroRNA-200 promotes lung cancer cell growth through FOG2-independent AKT activation. *International Union of Biochemistry and Molecular Biology Life*, 67. Doi: 10.1002/iub.1412

Guo, Y. J., Pan, W. W., Liu, S. B., et al. 2020. ERK/MAPK signalling pathway and tumorigenesis. *Experimental and Therapeutic Medicine*, 19. Doi: 10.3892/etm.2020.8454.

Hammami, W., Al-Thani, R., Fiori, S., Al-meer, S., et al. 2017. Patulin and patulin producing Penicillium spp. occurrence in apples and apple-based products including baby food. *The Journal of Infection in Developing Countries*, 11. DOI:10.3855/jidc.9043

Han, C., Bowen, W. C., Michalopoulos, G. K., et al. 2008. Alpha-1 adrenergic receptor transactivates signal transducer and activator of transcription-3 (Stat3) through activation of Src and epidermal growth factor receptor (EGFR) in hepatocytes. *Journal of Cellular Physiology*, 216. Doi:

10.1002/jcp.21420.

Harris, K. L., Bobe, G. & Bourquin, L. D. 2009. Patulin Surveillance in Apple Cider and Juice Marketed in Michigan. *Journal of Food Protection*, 72. DOI: 10.4315/0362-028x- 72.6.1255

Hays, A., Wissel, M., Colletti, K., et al. 2024. Recommendations for Method Development and Validation of qPCR and dPCR Assays in Support of Cell and Gene Therapy Drug Development. *The American Association of Pharmaceutical Scientists Journal*, 26. DOI: 10.1208/s12248-023-00880-9

Hong, S., Park, S. K., Lee, J., et al. 2023. Patulin Ameliorates Hypertrophied Lipid Accumulation and Lipopolysaccharide-Induced Inflammatory Response by Modulating Mitochondrial Respiration. *Antioxidants*, 12. https://doi.org/10.3390/antiox12091750Huan, H.-B., Wen, X.-D., Chen, X.-J., et al. 2017. Sympathetic nervous system promotes hepatocarcinogenesis by modulating inflammation through activation of alpha1-adrenergic receptors of Kupffer cells. *Brain, Behavior, And Immunity*, 59. Doi: 10.1016/j.bbi.2022.03.015.

Insel, P. A. 1989. Structure and Function of Alpha-Adrenergic Receptors. *The American Journal of Medicine*, 87. DOI: 10.1016/0002-9343(89)90108-3

Iqbal, S. Z., Malik, S., Asi, M. R., et al. 2018. Natural occurrence of patulin in different fruits, juices and smoothies and evaluation of dietary intake in Punjab, Pakistan. *Food Control*, 84. DOI: 10.1016/j.foodcont.2017.08.024

Iqbal, S. Z., Waseem, M., Abdull Razis, A. F., et al. 2024. Mycotoxin patulin contamination in various fruits and estimating its dietary impact on the consumers: From orchard to table. *Heliyon*, 10. Available: https://doi.org/10.1016/j.heliyon.2024.e30252

Isin, B., Estiu, G., Wiest, O., et al. 2013. Identifying Ligand Binding Conformations of the β2-Adrenergic Receptor by Using Its Agonists as Computational Probes. *PLOS ONE*, 7. Doi: 10.1371/journal.pone.0050186

Jayashree, G. V., Krupashree, K., Rachitha, P., et al. 2017. Patulin Induced Oxidative Stress Mediated Apoptotic Damage in Mice, and its Modulation by Green Tea Leaves. *Journal of Clinical and Experimental Hepatology*, 7. Doi: 10.1016/j.jceh.2017.01.113

Jiang, D., Cope, A. L., Zhang, J., et al. 2023. On the Decoupling of Evolutionary Changes in mRNA

and Protein Levels. *Molecular Biology and Evolution*, 40. Doi: 10.1093/molbev/msad169.

Jiang, N., Dai, Q., Su, X., et al. 2020. Role of PI3K/AKT pathway in cancer: the framework of malignant behavior. *Molecular Biology Reports*, 47. Doi: 10.1007/s11033-020- 05435-1.

Jin, H., Yin, S., Song, X., et al. 2016. p53 activation contributes to patulin- induced nephrotoxicity via modulation of reactive oxygen species generation. *Scientific Reports*, 6. Doi: 10.1038/srep24455.

Katerere, D., Stockenström, S., Thembo, K., et al. 2007. Investigation of patulin contamination in apple juice sold in retail outlets in Italy and South Africa. *Food additives and contaminants*, 24. DOI: 10.1080/02652030601137668

Kraft, S., Buchenauer, L. & Polte, T. 2021. Mould, mycotoxins and a dysregulated immune system: a combination of concern? *International Journal of Molecular Sciences*, 22. Doi: 10.3390/ijms222212269.

Kralik, P. & Ricchi, M. 2017. A basic guide to real time PCR in microbial diagnostics: definitions, parameters, and everything. *Frontiers in Microbiology*, 8. https://doi.org/10.3389/fmicb.2017.00108

Kumar, D., Tannous, J., Sionov, E., et al. 2018a. Apple Intrinsic Factors Modulating the Global Regulator, LaeA, the Patulin Gene. Accumulation during Fruit Colonization by Penicillium expansum. *Frontiers in Plant Science*, 9. Doi: 10.3389/fpls.2018.01094

Kumar, S., Chinnusamy, V. & Mohapatra, T. 2018b. Epigenetics of Modified DNA Bases: 5-Methylcytosine and Beyond. *Frontiers in Genetics*, 9. Doi: 10.3389/fgene.2018.00640

Kurdyukov, S. & Bullock, M. 2016. DNA Methylation Analysis: Choosing the Right Method. *Biology*, 5. Available: https://doi.org/10.3390/biology5010003

Leggott, N. L. & Shephard, G. S. 2001. Patulin in South African commercial apple products. *Food Control*, 12. DOI: 10.1016/S0956-7135(00)00023-2

Li, L., He, Z., Shi, Y., et al. 2023. Role of epigenetics in mycotoxin toxicity: A review. *Environmental Toxicology and Pharmacology*, 100. Doi: 10.1016/j.etap.2023.104154. Li, X., Tang, H., Yang, C., et al. 2019. Detoxification of mycotoxin patulin by the yeast Rhodotorula mucilaginosa. *Food Control*, 96, 47-52. DOI: 10.1016/J.FOODCONT.2018.08.029

Lin, A. V. 2015. Indirect ELISA. *Methods in Molecular Biology*, 1318. Doi: 10.1007/978-1-4939-2742- 5_5.Link, R., Daunt, D., Barsh, G., et al. 1992. Cloning of two mouse genes encoding alpha 2-adrenergic receptor subtypes and identification of a single amino acid in the mouse alpha 2-C10 homolog responsible for an interspecies variation in antagonist binding. *Molecular Pharmacology*, 42. PMID: 1353249

Liu, R., Chen, Y., Liu, G., et al. 2020. PI3K/AKT pathway as a key link modulates the multidrug resistance of cancers. *Cell Death & Disease*, 11. https://doi.org/10.1038/s41419-020-02998-6

Lytle, J. R., Yario, T. A. & Steitz, J. A. 2007. Target mRNAs are repressed as efficiently by microRNA-binding sites in the 5' UTR as in the 3' UTR. *Proceedings of the National Academy of Sciences of the United States of America*, 104. Doi: 10.1073/pnas.0703820104.

Mahmood, T. & Yang, P. C. 2012. Western blot: technique, theory, and trouble shooting. *North American Journal of Medicine and Science*, 4. Doi: 10.4103/1947-2714.100998

Martínez-Limón, A., Joaquin, M., Caballero, M., et al. 2020. The p38 pathway: from biology to cancer therapy. International Journal of Molecular Sciences, 21. Doi: 10.3390/ijms21061913

Mazibuko, M., Ghazi, T. & Chuturgoon, A. 2024. Patulin alters alpha-adrenergic receptor signalling and induces epigenetic modifications in the kidneys of C57BL/6 mice. *Archives of Toxicology*. 98. Doi: 10.1007/s00204-024-03728-z

McKinley, E. R., Carlton, W. W. & Boon, G. D. 1982. Patulin mycotoxicosis in the rat: Toxicology, pathology and clinical pathology. *Food and Chemical Toxicology*, 20.Available: DOI: 10.1016/s0278-6915(82)80295-0

Menezo, Y. J., Silvestris, E., Dale, B., et al. 2016. Oxidative stress and alterations in DNA methylation: two sides of the same coin in reproduction. *Reproductive BioMedicine*, 33. Doi: 10.1016/j.rbmo.2016.09.006.

Mishra, P., Pandey, C. M., Singh, U., et al.2019. Selection of Appropriate Statistical Methods for Data Analysis. *Annals of Cardiac Anaesthesia*, 22. PMID: 31274493Moon, H. & Ro, S. W. 2021. MAPK/ERK Signaling Pathway in Hepatocellular Carcinoma. *Cancers (Basel)*, 13. Doi: 10.3390/cancers13123026

Moss, M. O. 2008. Fungi, quality and safety issues in fresh fruits and vegetables. Journal of Applied Microbiology, 104. DOI: 10.1111/j.1365-2672.2007.03705.x

Mukherjee, R., Vanaja, K. G., Boyer, J. A., et al. 2021. Regulation of PTEN translation by PI3K signaling maintains pathway homeostasis. *Molecular Cell*, 81. Doi: 10.1016/j.molcel.2021.01.033.

Mulder, J. E., Bondy, G. S., Mehta, R., et al. 2015. The impact of chronic Aflatoxin B1 exposure and p53 genotype on base excision repair in mouse lung and liver. Mutation Research, 773. DOI: 10.1016/j.mrfmmm.2015.01.015

Nawaf, A. 2023. Mycotoxin source and its exposure causing mycotoxicoses. *Bioinformation*, 19. Doi: 10.6026/97320630019348

Nie, X., Fan, J., Li, H., et al. 2018. miR- 217 Promotes Cardiac Hypertrophy and Dysfunction by Targeting PTEN. *Molecular Therapy Nucleic Acids*, 12, . Doi: 10.1016/j.omtn.2018.05.013

Osswald, H., Frank, H. K., Komitowski, D. & Winter, H. 1976. Long-term testing of patulin administered orally to sprague-dawley rats and Swiss mice. *Food and Cosmetics Toxicology*, 16. https://doi.org/10.1016/S0015-6264 (76)80520-2

Pal, S., Singh, N. & Ansari, K. M. 2017. Toxicological effects of patulin mycotoxin on the mammalian system: an overview. *Toxicology Research (Camb)*, 6. Doi: 10.1039/c7tx00138

Pettinger, W. A. & Jackson, E. K. 2020. α (2)-Adrenoceptors: Challenges and Opportunities-Enlightenment from the Kidney. *Cardiovascular Therapeutics*, 2020. Doi: 10.1155/2020/2478781

Philipp, M., Brede, M. & Hein, L. 2002. Physiological significance of α2-adrenergic receptor subtype diversity: one receptor is not enough. *American Journal of Regulatory, Integrative and Comparative Physiology*, 283.Doi: 10.1152/ajpregu.00123.2002.

Pillay, Y., Nagiah, S., Phulukdaree, A., et al. 2020. Patulin suppresses α1-adrenergic receptor expression in HEK293 cells. Scientific Reports, 10. Doi: 10.1038/s41598-020-77157-0.

Pillay, Y., Phulukdaree, A., Nagiah, S., et al. 2015. Patulin triggers NRF2-mediated survival mechanisms in kidney cells. *Toxicon*, 99. Doi: 10.1016/j.toxicon.2015.03.004.

Puel, O., Galtier, P. & Oswald, I. P. 2010. Biosynthesis and toxicological effects of patulin. *Toxins (Basel)*, 2.DOI: 10.3390/toxins2040613

Qiu, Y., Chen, X., Chen, Z., et al. 2022. Effects of Selenium Nanoparticles on Preventing Patulin-

Induced Liver, Kidney and Gastrointestinal Damage. *Foods*, 11. Available: https://doi.org/10.3390/foods11050749

Rahmani, F., Ferns, G. A., Talebian, S., et al. 2020a. Role of regulatory miRNAs of the PI3K/AKT signalling pathway in the pathogenesis of breast cancer. *Gene*, 737. Doi: 10.1016/j.gene.2020.144459.

Rahmani, F., Ziaeemehr, A., Shahidsales, S., et al. 2020b. Role of regulatory miRNAs of the PI3K/AKT/mTOR signaling in the pathogenesis of hepatocellular carcinoma. *Journal of Cellular Physiology*, 235. Doi: 10.1002/jcp.29333.

Raistrick, H. 1943. Patulin in the common cold collaborative research on a derivative of penicillium patulum bainier: I. Introduction. *The Lancet*, 242.DOI: 10.1016/S0140- 6736(00)88176-3

Ramalingam, S., Bahuguna, A. & Kim, M. 2019. The effects of mycotoxin patulin on cells and cellularcomponents.*TrendsinFoodScience&Technology*,83.Available: https://doi.org/10.1016/j.tifs.2018.10.010

Reddy, C. S., Chan, P. K. & Hayes, A. W. 1978. Teratogenic and dominant lethal studies of patulin in mice. *Toxicology*, 11. DOI: 10.1016/s0300-483x (78)91339-2

Saleh, I. & Goktepe, I. 2019. The characteristics, occurrence, and toxicological effects of patulin. *Food and Chemical Toxicology*, 129. Doi: 10.1016/j.fct.2019.04.036.

Schwinghammer, U. A., Melkonyan, M. M., Hunanyan, L., et al. 2020. α2-Adrenergic Receptor in Liver Fibrosis: Implications for the Adrenoblocker Mesedin. *Cells*, 9. Doi: 10.3390/cells9020456

Schütze, N., Lehmann, I., Bönisch, U., et al. 2010. Exposure to Mycotoxins Increases the Allergic Immune Response in a Murine Asthma Model. *American Journal of Respiratory and Critical Care Medicine*, 181.DOI: 10.1164/rccm.200909-1350O

Segal, M. & Slack, F. J. 2020. Challenges identifying efficacious miRNA therapeutics for cancer. *Expert Opinion on Drug Discovery*, 15. Doi: 10.1080/17460441.2020.1765770

Selmanoğlu, G. 2006. Evaluation of the reproductive toxicity of patulin in growing male rats. *Food and Chemical Toxicology*, 44. https://doi.org/10.1016/j.fct.2006.06.022

Shamsan, E., Almezgagi, M., Gamah, M., et al. 2024. The role of PI3k/AKT signaling pathway in attenuating liver fibrosis: a comprehensive Review. Frontiers in Medicine *(Lausanne)*, 11. Doi: 10.3389/fmed.2024.1389329.

Shephard, G. S., Van Der Westhuizen, L., Katerere, D. R., et al. 2010. Preliminary exposure assessment of deoxynivalenol and patulin in South Africa. *Mycotoxin Research*, 26. Doi: 10.1007/s12550-010-0052-9.

Shu, F., Xiao, H., Li, Q.-N., et al. 2023. Epigenetic and post-translational modifications in autophagy: biological functions and therapeutic targets. *Signal Transduction and Targeted Therapy*, 8. Available: https://doi.org/10.1038/s41392-022-01300-8

Soler, L. & Oswald, I. P. 2018. The importance of accounting for sex in the search of proteomic signatures of mycotoxin exposure. Journal of Proteomics, 178. Doi: 10.1016/j.jprot.2017.12.017.

Strader, C. D., Dixon, R. A., Cheung, A. H., et al. 1987. Mutations that uncouple the beta-adrenergic receptor from Gs and increase agonist affinity. Journal of Biological Chemistry, 262. PMID: 2890637

Strader, C. D., Gaffney, T., Sugg, E. E., Candelore, M. R., Keys, R., Patchett, A. A. & Dixon, R. A. 1991. Allele-specific activation of genetically engineered receptors. *Journal of Biological Chemistry*, 266. PMID: 1670767

Strosberg, A. D. 1993. Structure, function, and regulation of adrenergic receptors. *Protein Science*, 2. Doi: 10.1002/pro.5560020802.

Sugiyama, K. I., Kinoshita, M., Furusawa, H., et al. 2021. Epigenetic effect of the mycotoxin fumonisin B1 on DNA methylation. *Mutagenesis*, 36. Doi: 10.1093/mutage/geab019.

Sule, R., Rivera, G. & Gomes, A. V. 2023. Western blotting (immunoblotting): history, theory, uses, protocol and problems. *BioTechniques*, 75. Doi: 10.2144/btn-2022-0034

Tao, X., Chen, C., Chen, Y., et al. 2022. β2-adrenergic receptor promotes liver regeneration partially through crosstalk with c-met. *Cell Death Dis*., 13. Doi: 10.1038/s41419-022-04998-0.

Torović, L., Dimitrov, N., Assunção, R., et al. 2017. Risk assessment of patulin intake through apple-based food by infants and preschool children in Serbia. *Food additives & contaminants. Part A, Chemistry, analysis, control, exposure & risk assessment*, 34. Doi: 10.1080/19440049.2017.1364434

Torović, L., Dimitrov, N., Lopes, A., Martins, C., Alvito, P. & Assunção, R. 2018. Patulin in fruit juices: occurrence, bioaccessibility, and risk assessment for Serbian population. *Food additives & contaminants. Part A, Chemistry, analysis, control, exposure & risk assessment*, 35.Doi: 10.1080/19440049.2017.1419580

Trebicka, J., Hennenberg, M., Schulze Pröbsting, A., et al. 2009. Role of β3-adrenoceptors for intrahepatic resistance and portal hypertension in liver cirrhosis. *Hepatology*, 50. Doi: 10.1002/hep.23222.

Tu, K., Liu, Z., Yao, B., et al. 2016. MicroRNA-519a promotes tumor growth by targeting PTEN/PI3K/AKT signaling in hepatocellular carcinoma. *International Journal of Oncology*, 48. Doi: 10.3892/ijo.2015.3309.

Vaclavikova, M., Dzuman, Z., Lacina, O., et al. 2015. Monitoring survey of patulin in a variety of fruit-based products using a sensitive UHPLC–MS/MS analytical procedure. *Food Control*, 47. DOI: 10.1016/j.foodcont.2014.07.064

Vasudevan, N. T., Mohan, M. L., Goswami, S. K. et al. 2011. Regulation of β- adrenergic receptor function: an emphasis on receptor resensitization. *Cell Cycle*, 10
~~91~~. Doi: 10.4161/cc.10.21.18042.

Vinken, M., Doktorova, T., Decrock, E., et al. 2009. Gap junctional intercellular communication as a target for liver toxicity and carcinogenicity. *Critical Reviews in Biochemistry and Molecular Biology*.44. Doi: 10.1080/10409230903061215.

Vaclavikova, M., Dzuman, Z., Lacina, O., et al. 2015. Monitoring survey of patulin in a variety of fruit-based products using a sensitive UHPLC–MS/MS analytical procedure. *Food Control*, 47. DOI: 10.1016/j.foodcont.2014.07.064

Vasudevan, N. T., Mohan, M. L., Goswami, S. K. et al. 2011. Regulation of β- adrenergic receptor function: an emphasis on receptor resensitization. *Cell Cycle*, 10
. Doi: 10.4161/cc.10.21.18042.

Vinken, M., Doktorova, T., Decrock, E., Leybaert, L., Vanhaecke, T. & Rogiers, V. 2009. Gap junctional intercellular communication as a target for liver toxicity and carcinogenicity. *Critical Reviews in Biochemistry and Molecular Biology*, 44. Doi: 10.1080/10409230903061215.

Wan, J., Ling, X., Peng, B., et al. 2018. miR-142-5p regulates CD4+ T cells in human non- small cell lung cancer through PD-L1 expression via the PTEN pathway. *Oncology Reports*, 40. Doi: 10.3892/or.2018.6439

Wang, J., Li, H., Qiu, S., et al. 2017. MBD2 upregulates miR-301a- 5p to induce kidney cell apoptosis during vancomycin-induced AKI. *Cell Death & Disease*, 8. Doi: 10.1038/cddis.2017.509.

Wei, C., Yu, L., Qiao, N., et al. 2020. Progress in the distribution, toxicity, control, and detoxification of patulin: A review. *Toxicon*, 184. Doi: 10.1016/j.toxicon.2020.05.006

Wen, X., Jiao, L. & Tan, H. 2022. MAPK/ERK Pathway as a central regulator in vertebrate organ regeneration. *International Journal of Molecular Sciences*, 23. Doi: 10.3390/ijms23031464

Wilhelm, J. & PINGOUD, A. 2003. Real-Time Polymerase Chain Reaction. *ChemBioChem*, 4. Doi: 10.1002/cbic.200300662.

World Health Organisation (WHO). 2011. *FAO/WHO guide for application of risk analysis principles and procedures during food safety emergencies*. Rome: Food and Agriculture Organization of the United Nations. & World Health Organisation.

World Health Organisation (WHO). 2023. *Mycotoxins*. Available: https://www.who.int/news-room/fact-sheets/detail/mycotoxins [Accessed 28 November 2024].

Wu, Y., Fan, X., Yu, H., et al. 2022. Macrophage polarization is involved in liver fibrosis induced by β (1)-adrenoceptor autoantibody. *Acta Biochimica et Biophysica Sinica (Shanghai)*, 54. Doi: 10.3724/abbs.2022102.

Wu, Y., Zeng, L. & Zhao, S. 2021. Ligands of adrenergic receptors: a structural point of view. *Biomolecules*, 11. Doi: 10.3390/biom11070936.

Xue, C., Li, G., Lu, J., et al. 2021. Crosstalk between circRNAs and the PI3K/AKT signaling pathway in cancer progression. *Signal Transduction and Targeted Therapy*, 6, 400. Doi: 10.1038/s41392- 021-00788-w.

Yang, Y., Yang, Y., Shao, B., et al. 2017. A simple and rapid method for determination of patulin in juice by high performance liquid chromatography tandem mass spectrometry. *Food Analytical Methods*, 10. DOI: 10.1007/s12161-017-0859-5

Zapater, P., Gómez-Hurtado, I., Peiró, G., et al. 2012. Beta-Adrenergic Receptor 1 selective antagonism inhibits norepinephrine-mediated TNF-alpha downregulation in experimental liver cirrhosis. *PLOS ONE*, 7. Doi: 10.1371/journal.pone.0043371

Zhang, B., Peng, X., Li, G., et al. 2015. Oxidative stress is involved in Patulin induced apoptosis in

HEK293 cells. *Toxicon*, 94. Doi: 10.1016/j.toxicon.2014.12.002.

Zheng, X., Li, Y., Zhang, H., et al. 2018. Identification and toxicological analysis of products of patulin degradation by Pichia caribbica. *Biological Control*, 123. DOI: 10.1016/j.biocontrol.2018.04.019

Zhong, L., Carere, J., Lu, Z., et al. 2018. Patulin in apples and apple-based food products: the burdens and the mitigation strategies. *Toxins (Basel)*, 10. Available: https://doi.org/10.3390/toxins10110475

Zhu, C. C., Hou, Y. J., Han, J., et al. 2014. Effect of mycotoxin-containing diets on epigenetic modifications of mouse oocytes by fluorescence microscopy analysis. *Microscopy and Microanalysis*, 20. DOI: 10.1017/S1431927614000919

Appendix A: Ethics Approval Letter

UNIVERSITY OF KWAZULU-NATAL
INYUVESI YAKWAZULU-NATALI

18 September 2018

Professor Anil Chuturgoon (34866)
School of Laboratory Medicine & Medical Sciences
Howard College Campus

Dear Professor Chuturgoon,

Protocol reference number: AREC/079/016
Project title: The molecular and epigenetic effects of selected mycotoxins on C57B/6 black mice

Full Approval – Renewal Application

With regards to your renewal application received on 24 August 2018. The documents submitted have been accepted by the Animal Research Ethics Committee and **FULL APPROVAL** for the protocol has been granted.

Please note: Any Veterinary and Para-Veterinary procedures must be conducted by a SAVC registered VET or SAVC authorized person.

Any alteration/s to the approved research protocol, i.e Title of Project, Location of the Study, Research Approach and Methods must be reviewed and approved through the amendment/modification prior to its implementation. In case you have further queries, please quote the above reference number.

Please note: Research data should be securely stored in the discipline/department for a period of 5 years.

The ethical clearance certificate is only valid for a period of one year from the date of issue. Renewal for the study must be applied for before 18 September 2019.

Attached to the Approval letter is a template of the Progress Report that is required at the end of the study, or when applying for Renewal (whichever comes first). An Adverse Event Reporting form has also been attached in the event of any unanticipated event involving the animals' health / wellbeing.

I take this opportunity of wishing you everything of the best with your study.

Yours faithfully

[redacted]

Professor S Islam, PhD
Chair: Animal Research Ethics Committee

/ms

Cc Acting Academic Leader Research: Dr Brenda de Gama
Cc Registrar: Mr Simon Mokoena
Cc NSPCA: Ms Anita Engelbrecht
Cc BRU – Dr Linda Bester

Animal Research Ethics Committee (AREC)
Ms Mariette Snyman (Administrator)
Westville Campus, Govan Mbeki Building
Postal Address: Private Bag X54001, Durban 4000
Telephone: +27 (0) 31 260 8350 **Facsimile:** +27 (0) 31 200 4009 **Email:** animalethics@ukzn.ac.za
Website: http://research.ukzn.ac.za/Research-Ethics/Animal-Ethics.aspx

Appendix B: ELISA

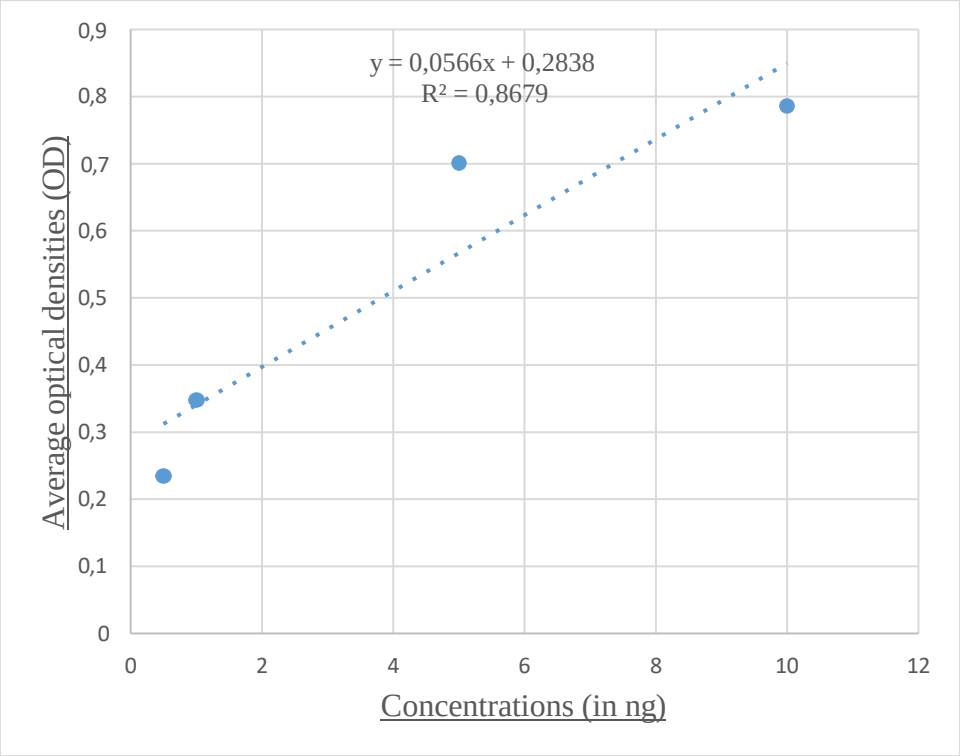

Figure 5: The standard curve illustrating 5-mC concentrations (ng) against average optical densities (OD)

Appendix C: BCA assay

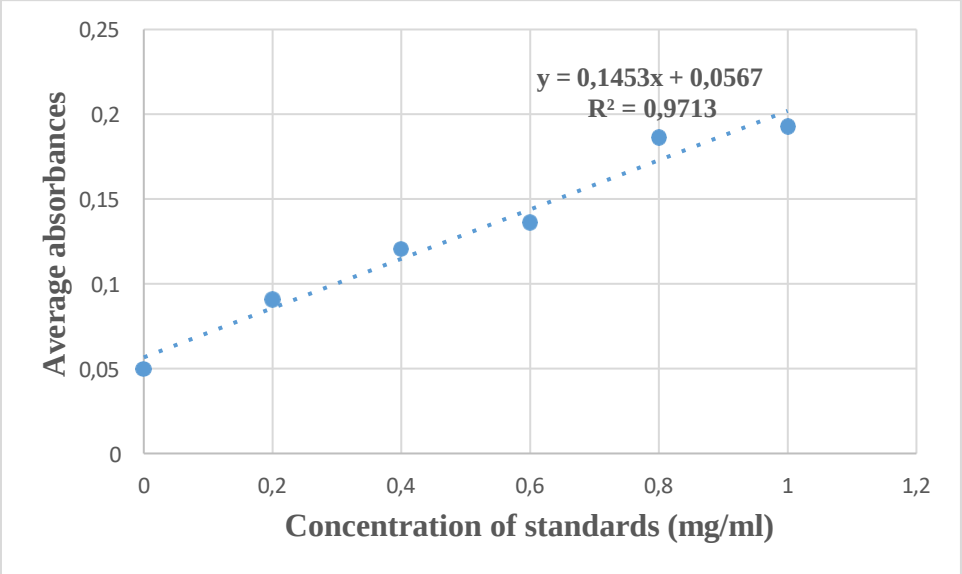

Figure 6: The BCA assay standard curve illustrating concentration standards (mg/ml) against average absorbances

Appendix D: Omitted results

A ten-eleven translocation (TET) family enzyme namely 2-oxoglutarate-dependent-cytosine-dioxygenase facilitates active DNA demethylation by oxidatively altering cytosine (Bind et al., 2022). The TET enzymes convert 5-mC into 5-hydroxymethylcytosine (5-HmC), 5- formylcytosine (5-fC), and 5-carboxylcytosine (5-caC) via oxidation processes. These altered bases could be DNA demethylation intermediates (Menezo et al., 2016). DNA demethylation requires 5-HmC, a product of oxidised cytosine. Oxidised cytosine is either degraded by enzymes or eliminated during replication (Bind et al., 2022).

Utilising the qPCR assay, the mRNA levels of TET 1, 2 and 3 were investigated.

Table 5: TET primer sequences purchased from Inqaba Biotechnical

TET 1	58°C	F: ACACAGTGGTGCTAATGCAG R: AGCATGAACGGGAGAATCGG
TET 2	58°C	F: AGAGAAGACAATCGAGAAGTCGG R: CCTTCCGTACTCCCAAACTCAT
TET 3	58°C	F: GTGGTCGGACAGTGAACACAA R: GTTGGGCTGGTTGAGGTTCTT

PAT increased the levels of *TET 1* (p = 0,3485) (Figure 7a), significantly increased *TET 2* (p<0.0001) (Figure 7b), whilst significantly decreasing *TET 3* (p = 0,0326) (Figure 7c).

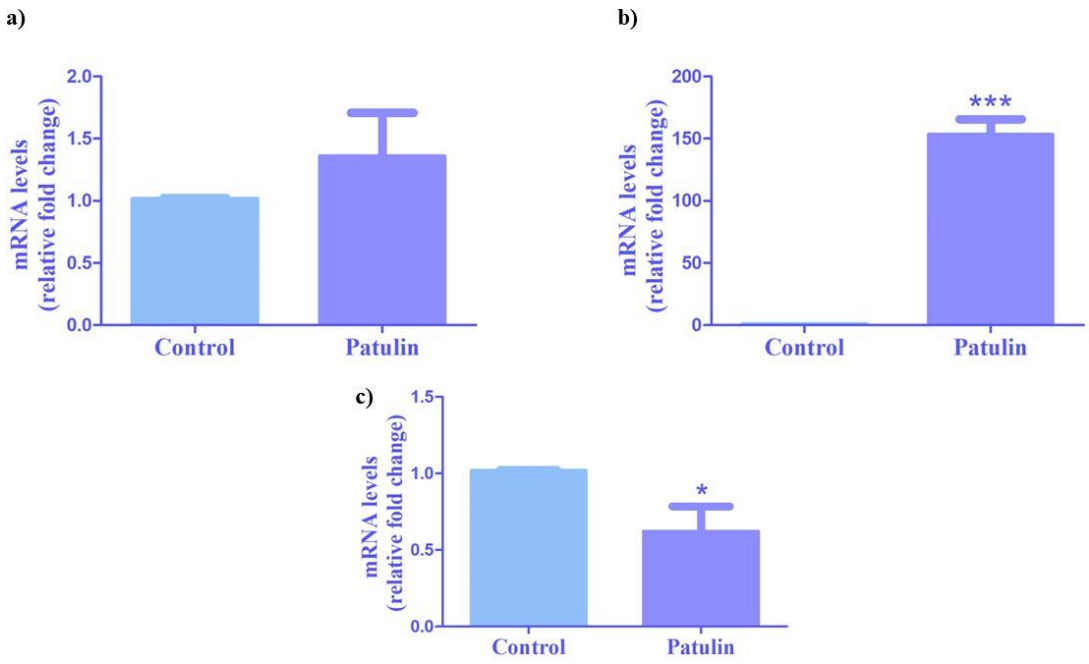

Figure 7: The mRNA levels of the TET proteins a) *TET1*, b) *TET2* and c) *TET3*. All data is represented as mean with SEM where (*p<0.05, ***p<0.0001) was deemed significant.

The mRNA levels of *TET1* were not significantly increased. PAT however significantly increased and decreased *TET2* and *TET3* respectively.

Appendix E: Summary Comparison Table

Table 6: The different effects of PAT on adrenergic receptor signalling and global DNA methylation in the kidney and the liver of C57BL/6 mice

	The effects of 10-day PAT administration in the kidney	The effect of 10-day PAT administration in the liver
α1A-AR	Significant ↓ mRNA levels	Significant ↑ mRNA levels
α2A-AR	Significant ↓ mRNA levels	↓ mRNA levels
α2B-AR	Significant ↓ mRNA levels	↓ mRNA levels
β1	N/A	↓ mRNA levels
β2	N/A	Significant ↓ mRNA levels
β3	N/A	↓ mRNA levels
MAPK	Significant ↑mRNA levels Significant ↑ protein expression	Significant ↑ mRNA levels
MAPK14	Significant ↑ increased mRNA levels	Significant ↑ mRNA levels
P38	N/A	Significant ↑ protein levels
ERK 1	N/A	Significant ↑ mRNA levels
ERK 2	N/A	Significant ↓ mRNA levels
ERK 1/2	Significant ↑ protein expression	Significant ↓ protein expression.

PI3K	Significant ↓ mRNA levels	↓ mRNA levels Significant ↑ protein expression
AKT	Significant ↑ mRNA levels	Significant ↑ mRNA levels
DNMT 1	Significant ↑ mRNA levels	↑ mRNA levels Significant ↑ in protein levels
DNMT 3A	Significant ↓ mRNA levels	Significant ↓ mRNA levels ↑ protein expression
DNMT 3B	Significant ↓ mRNA levels	Significant ↓ mRNA levels
MBD2	Significant ↑ mRNA levels	↑ mRNA levels and protein expression
GLOBAL DNA METHYLATION	Significant ↓ in global DNA methylation levels (hypomethylation)	Significant ↑ in global DNA methylation levels (hypermethylation)